

Article

## Identification of High-potency Human TLR8 and Dual TLR7/TLR8 Agonists in Pyrimidine-2,4-diamines

Mallesh Beesu, Alex C. D. Salyer, Michael J. H. Brush, Kathryn L. Trautman, Justin K. Hill, and Sunil A. David

*J. Med. Chem.*, **Just Accepted Manuscript** • DOI: 10.1021/acs.jmedchem.6b01860 • Publication Date (Web): 01 Feb 2017

Downloaded from <http://pubs.acs.org> on February 1, 2017

### Just Accepted

"Just Accepted" manuscripts have been peer-reviewed and accepted for publication. They are posted online prior to technical editing, formatting for publication and author proofing. The American Chemical Society provides "Just Accepted" as a free service to the research community to expedite the dissemination of scientific material as soon as possible after acceptance. "Just Accepted" manuscripts appear in full in PDF format accompanied by an HTML abstract. "Just Accepted" manuscripts have been fully peer reviewed, but should not be considered the official version of record. They are accessible to all readers and citable by the Digital Object Identifier (DOI®). "Just Accepted" is an optional service offered to authors. Therefore, the "Just Accepted" Web site may not include all articles that will be published in the journal. After a manuscript is technically edited and formatted, it will be removed from the "Just Accepted" Web site and published as an ASAP article. Note that technical editing may introduce minor changes to the manuscript text and/or graphics which could affect content, and all legal disclaimers and ethical guidelines that apply to the journal pertain. ACS cannot be held responsible for errors or consequences arising from the use of information contained in these "Just Accepted" manuscripts.

1  
2  
3  
4  
5  
6  
7  
8  
9  
10  
11  
12  
13  
14  
15  
16  
17  
18  
19  
20  
21  
22  
23  
24  
25  
26  
27  
28  
29  
30  
31  
32  
33  
34  
35  
36  
37  
38  
39  
40  
41  
42  
43  
44  
45  
46  
47  
48  
49  
50  
51  
52  
53  
54  
55  
56  
57  
58  
59  
60

# Identification of High-potency Human TLR8 and Dual TLR7/TLR8 Agonists in Pyrimidine-2,4-diamines

**Mallesh Beesu, Alex C. D. Salyer, Michael J. H. Brush, Kathryn L. Trautman, Justin K. Hill, and Sunil A. David\***

Department of Medicinal Chemistry,  
University of Minnesota, Minneapolis, MN 55455, USA.

**Running Title:** Dual TLR7/TLR8 agonism in substituted pyrimidine-2,4-diamines

**Keywords:** TLR7, TLR8, TLR7/8 agonists, Pyrimidine-2,4-diamines, Vaccine adjuvants, Innate immunity.

## Abstract

The induction of Toll-like receptor 7 (TLR7)-dependent Type I interferons (IFN- $\alpha/\beta$ ) from plasmacytoid dendritic cells as well as the production of TLR8-dependent Type II interferon (IFN- $\gamma$ ), TNF- $\alpha$ , and IL-12 in myeloid dendritic cells are of importance in generating T helper-1 biased adaptive immune responses. In an effort to identify novel dual TLR7/TLR8-active compounds, we undertook structure-activity relationship studies in pyrimidine 2,4-diamines, focusing on substituents at C5. Several analogues substituted with aminopropyl appendages at C5 displayed dominant TLR8-agonistic activity. *N*<sup>4</sup>-butyl-6-methyl-5-(3-morpholinopropyl) pyrimidine-2,4-diamine was found to be a very potent dual TLR7/TLR8 agonist. Employing novel cytokine reporter cell assays, we verified that potency at TLR7 correlates with IFN- $\alpha/\beta$  production in human blood, whereas IFN- $\gamma$  and TNF- $\alpha$  induction are largely TLR8-dependent. Dual TLR7/TLR8 agonists markedly upregulate CD80 expression in multiple dendritic cell subsets, providing insight into the immunological basis for the superior adjuvant properties of such innate immune stimuli.

(144 words)

Introduction

Vaccination against infectious diseases has greatly reduced disease burden around the globe and has served as an important means of promoting human health.<sup>1, 2</sup> Effective vaccines for a large number of infectious diseases are yet to be developed, not only for diseases of enormous consequence to global health such as malaria, tuberculosis, and HIV/AIDS, but also to newly emerging pathogens such as Zika, Dengue, and Chikungunya viruses.<sup>3-7</sup>

The mobilization of immune responses to pathogens has traditionally been compartmentalized into innate and adaptive components.<sup>8, 9</sup> The adaptive component is comprised mainly of two classes of specialized cells—B and T lymphocytes. Individual cells in both these classes of lymphocytes display structurally unique, antigen-specific receptors. The very large and diverse repertoire of antigen receptors enables the specific lymphocyte whose receptor specifically recognizes epitope(s) on the antigen to become activated and proliferate. This process, termed clonal selection, endows the adaptive immune system to respond specifically to a given pathogen. However, the processes of clonal expansion and differentiation into effector cells take several days to be mobilized.

The effector mechanisms of the innate component of immunity, in contrast, are brought into play immediately upon injury or infection, and it is becoming increasingly clear that not only are innate immune responses essential for the induction and augmentation of the tardy, but specific adaptive immune responses, but the nature of innate immune signals can shape downstream adaptive responses.<sup>8, 10, 11</sup> This is of particular significance in the design and

development of vaccines, especially given that the majority of modern subunit vaccines utilize highly purified, recombinantly expressed proteins which, by themselves are often negligibly immunogenic, and therefore depend on vaccine adjuvants<sup>12-15</sup> (substances that enhance immune responses) to provide the initial innate immune-activating signals that determine the specificity, magnitude, quality, and durability of adaptive immune responses.

Important among signals originating in the innate immune system are those that arise from Toll-like receptors (TLRs);<sup>16</sup> the 10 functional TLRs in the human serve as pattern-recognition receptors (PRRs) which recognize pathogen-associated molecular patterns (PAMPs).<sup>17, 18</sup> The TLRs share a modular structure, characterized by the presence of an extramembranous ectodomain which bear repeating blocks of a ~24-amino-acid motif called a leucine-rich repeat (LRR); the PAMP-sensing ectodomain is connected to the signal-transducing cytosolic domain via a membrane-spanning long  $\alpha$ -helix.<sup>19</sup> TLRs reside either on the cell membrane, or in intracellular compartments and are thereby specialized to recognize signals from extracellular or intracellular pathogens. TLR1, -2, -4, -5, and -6 recognize extracellular stimuli, while TLR3, -7, -8 and -9 function within the endolysosomal compartment.<sup>20-22</sup> The ligands for TLRs are highly conserved molecules such as lipopolysaccharides (LPS) and monophosphoryl lipid A (MPLA) (recognized by TLR4), lipopeptides (TLR2 in combination with TLR1 or TLR6), flagellin (TLR5), single stranded RNA (TLR7 and TLR8), double stranded RNA (TLR3), and CpG motif-containing single-stranded DNA (recognized by TLR9).<sup>22, 23</sup>

Although our understanding of efferent immune responses in response to a variety of innate immune stimuli has increased tremendously over the past decade, questions remain about

how we can rationally utilize these stimuli in the design and development of vaccine adjuvants. Our research program has emphasized the detailed exploration of structure-activity relationships in small molecule agonists of TLR2,<sup>24-26</sup> TLR4,<sup>27, 28</sup> TLR7,<sup>29-37</sup> TLR8,<sup>38-46</sup> NOD1,<sup>47</sup> and C-C chemokine receptor type 1 (CCR1)<sup>48</sup> with a view to identifying effective vaccine adjuvants with minimal reactogenicity.

We have, in particular, focused our attention on adjuvants capable of eliciting T helper-1 (Th1) responses.<sup>49-51</sup> Discovered nearly 30 years ago, the biphasic model of Th1/Th2 responses has now grown to include Th17, Th9, T follicular-helper (Tfh), and T-regulatory (Treg) CD4<sup>+</sup> lymphocyte subsets,<sup>52</sup> and whilst a detailed discussion of the immunology of Th cell subsets is beyond the scope of this paper, it is pertinent to note that the induction of undesirable, hypersensitivity-mediating immunoglobulin E (IgE) responses has long been associated with Th2-skewed immunity.<sup>50</sup>

In the context of Th1-biased adaptive immune responses, both TLR7 and TLR8 are of significance. Plasmacytoid dendritic cells (pDCs), in particular, express TLR7, and its occupancy leads to the induction of copious quantities of Type I interferons (IFN- $\alpha/\beta$ )<sup>53-55</sup> contributing to Th1-polarized responses,<sup>56</sup> influencing not only the fate of CD4<sup>+</sup> and CD8<sup>+</sup> T cells during the initial phases of antigen recognition, but also defining the generation of effector and memory T-cell pools.<sup>57</sup> Furthermore, Type I IFNs appear to suppress Th2 and Th17 responses.<sup>57</sup> The engagement of TLR8, expressed predominantly in myeloid dendritic cells (mDCs) which are also referred to as conventional dendritic cells (cDCs), monocytes, and monocyte-derived dendritic cells,<sup>58, 59</sup> potentially enhances the production of Th1-polarizing cytokines, TNF- $\alpha$ , IL-12,

and IL-18 in APCs.<sup>58, 60-62</sup>

Concurrent engagement of TLR7 and TLR8, and consequent induction of Type I interferons, as well as Th1-polarizing cytokines may therefore be likely to strongly influence the development of Th1-biased immunity. Indeed in evaluating nearly 50 candidate adjuvants embodying diverse chemotypes and targeting a variety of TLRs<sup>24-26, 29-48, 59, 63, 64</sup> in a standardized rabbit model of immunization during the last several years, we have found that dual TLR7/8 agonists significantly outperform equipotent pure TLR7 and pure TLR8 agonists (manuscript in preparation; structures of key compounds are shown in Fig. 1). Of the several dual TLR7/8 agonists that we examined,<sup>32, 36</sup> we have flagged a number of compounds such as **1f** and **1g** (Fig. 1) owing to potential reactogenicity (induction of C-reactive protein and/or hyperthermia in rabbits at supraphysiological doses; manuscript in preparation), and two imidazoquinolines analogues<sup>65</sup> (**1c**, **1d**, Fig. 1) that we had originally characterized have emerged as lead dual TLR7/8-active, candidate vaccine adjuvants.

In an effort to identify novel dual TLR7/TLR8-active compounds, we continued structure-activity relationship studies in pyrimidine diamines. We report in this paper the identification of several high-potency TLR8 agonists, as well as a dual TLR7/TLR8 agonist.

## Results and Discussion

Our point of departure in these studies was the *N*<sup>4</sup>-butyl-6-methylpyrimidine-2,4-diamine scaffold, which had been identified as a hit in a multiplexed, reporter gene-based high-throughput screen,<sup>27</sup> and on which structure-activity relationship studies had been reported by us<sup>39</sup> and others.<sup>66</sup> In our earlier study, we had explored substituents on C5, and had found that a 5-butylamine-substituted analogue (**1n**, Fig. 1) yielded a pure human TLR8 agonist with a potency of 300 nM.<sup>39</sup> Noting from this earlier study that substituents at C5 greatly impacted activity,<sup>39</sup> we sought to explore in greater detail additional analogues. We began by examining a congeneric series of 5-alkyl-substituted *N*<sup>4</sup>-butyl-6-methylpyrimidine-2,4-diamines (Scheme 1). Compound **3** (5-methyl), **6a** (5-ethyl), and **6b** (5-butyl) were synthesized via S<sub>N</sub>Ar reactions from 4-Chloro intermediates (Scheme 1), while **11a** (5-pentyl) was obtained via Sonogashira coupling of the 5-iodo intermediate **9**, with 1-pentyne, and subsequent hydrogenation (Scheme 2). In contrast to pure TLR8-agonistic activity observed previously in 5-iodo- or 5-alkylamino-substituted *N*<sup>4</sup>-butyl-6-methylpyrimidine-2,4-diamine,<sup>39</sup> we noticed the emergence of weak dual TLR7/8 agonistic activity in these compounds (Table 1), prompting a more detailed and systematic exploration.

Bioisosteric replacement of the ω-amine at C5 in our previous lead with a primary alcohol (**11b**) or tertiary alcohol-bearing analogues (**11c**, **11d**), accessed via Sonogashira coupling (Scheme 2), did not lead to substantial changes in either TLR7- or TLR8-agonistic potencies (Table 1). In an effort to augment potency at TLR7, we sought to apply SAR information gleaned from our earlier work on imidazoquinolines<sup>32, 36</sup> and imidazopyridines,<sup>37</sup> in both these chemotypes, strategically-placed aromatic groups were found to be pivotal in



conferring selectivity at TLR7, presumably via  $\pi$ - $\pi$  interactions. The 5-pent-1-yne-substituted analogue **10a** (a precursor of **11a**, Scheme 2) as well as the 5-ethynyl analogue **13** (and its trimethylsilyl-substituted precursor **12**, Scheme 2) were, disappointingly, devoid of TLR7-stimulatory activity (Table 1). We attempted homologation of the 5-benzyl substituent (**14a**) which we had previously shown to be inactive at TLR7 and weakly active at TLR8 ( $EC_{50}$ : 1.2  $\mu$ M).<sup>39</sup> The homologous series of 5-phenethyl (**14b**), 5-phenylpropyl (**17a**), 5-phenylbutyl (**17b**), and 5-phenylpentyl (**17c**) were therefore synthesized. Suzuki coupling of the 5-iodo intermediate **9** with 2-phenylvinylboronic acid (Scheme 3) yielded **14b**, while compounds **17a-c** were accessed via Sonogashira coupling (Scheme 4). Compound **17a** with a 5-phenylpropyl substituent was found to be optimal with  $EC_{50}$  values of 0.19 and 0.75  $\mu$ M at human TLR7 and TLR8, respectively. A ten-fold decrease in TLR7-agonistic potency ( $EC_{50}$ : 1.1  $\mu$ M) and a complete loss of TLR8-stimulatory activity in the 5-cyclohexylpropyl analogue **17d** appeared to substantiate the premise that  $\pi$ - $\pi$  interactions were crucial, and that a trimethylene spacer was optimal. We therefore examined several heteroaromatic substitutions at C5, including pyrazolylpropyl (**17e**), 1,2,4-triazolylpropyl (**17f**), indolylpropyl (**17g**), 2-methyl-benzo[*d*]imidazolylpropyl (**17h**), propyl-isoindoline-1,3-dione (**17i**) and propyl-isoindoline (**17j**) analogues (Scheme 4). Among these analogues, the 2-methyl-benzo[*d*]imidazolylpropyl-substituted **17h** showed near-equipotent agonistic activity for both TLR7 and TLR8 ( $EC_{50}$ : 0.38 and 0.37  $\mu$ M, respectively), surpassing the most potent dual TLR7/TLR8-active pyrimidine diamine compound recently reported by McGowan and colleagues ( $EC_{50}$ : >1.6  $\mu$ M, for both TLR7 and TLR8).<sup>66</sup>

To our surprise, we noted that the phthalimide (isoindoline-1,3-dione)-bearing analogue **17i** retained substantial dual TLR7/8 activity, while in the isoindoline substituted derivative **17j**,

TLR7 agonistic activity was maintained and TLR8-stimulatory potency increased approximately eight-fold ( $EC_{50}$ : 29 nM), relative to **17h**, leading us to re-examine our premise of  $\pi$ - $\pi$  interactions driving potency. We therefore evaluated the pyrrolidinylpropyl analogue **17k**, which could be considered a part-structure of **17j**. The preservation of dual TLR7/TLR8 agonism in this compound argued against our conjecture that aromatic substituents were necessary, setting us on a path toward exploring the ring-expanded piperidinylpropyl (**17l**) and azepanylpropyl (**17m**) analogues, as well as the non-cycloaliphatic amine-bearing analogues **17n** and **17o** (Scheme 4). TLR8-agonistic activity was retained in all of these analogues (Table 1), but significant attenuation in maximal responses in TLR7 agonism assays were noted (see discussion on  $R_{max}$  values, below, and Fig. 2a) in **17l**, **17m** and **17n**, and a complete loss of TLR7-stimulatory activity was observed for **17o**. These results appeared to suggest that cycloaliphatic substituents possessing additional H-bond donor/acceptor atoms could favor TLR7 engagement.

In a final salvo, we therefore explored di-heteroatom-containing saturated heterocyclic substituents, including piperazinyl (**17p-17s**) and thiomorpholinyl (**17t**) analogues. The Boc-protected piperazinyl compound **17p** was found to be a potent pure TLR8 agonist, whereas the **17q**, **17r**, **17s** and **17t** were dual TLR7/TLR8-active. These results appeared to suggest that the replacement of the H-bond donor in the piperazinyl analogue **17q** to an H-bond acceptor could be beneficial, and we therefore synthesized the morpholinyl analogue (**17u**; Scheme 4). This proved to be correct, and compound **17u** was found to be very potent for both TLR7 ( $EC_{50}$ : 46 nM) and TLR8 ( $EC_{50}$ : 280 nM), whereas the thiomorpholinyl analogue **17t** was found to be considerably weaker at TLR7 ( $EC_{50}$ : 714 nM), pointing to the requirement of an appropriately electronegative H-bond donor atom. A substantial reduction in TLR7 activity ( $EC_{50}$ : 1240 nM) and unchanged TLR8 activity ( $EC_{50}$ : 203 nM) in the ‘ring-broken’ analogue **17v** points to

1  
2  
3 conformational restrictions inherent in the morpholinyl group contributing to potency at TLR7,  
4  
5 and a decrease in TLR7 potency ( $EC_{50}$ : 1400 nM) in the morpholinylbutyl homologue **17w**  
6  
7 confirmed that the propyl spacer was optimal.  
8  
9

10  
11 In the last several years that we have been characterizing TLR-active agents, a frequent  
12  
13 observation<sup>39, 42, 46</sup> has been that analogues differ substantially not only in their  $EC_{50}$  values in  
14  
15 dose-response curves, but also in the maximal responses ( $R_{max}$ ) in TLR-specific reporter gene  
16  
17 assays. Similar to our observations in the past, differences in  $R_{max}$  values are also observed in  
18  
19 some of the pyrimidine diamines (for instance the maximal responses for TLR7 activity are in  
20  
21 the order: **17u** > **17a** >> **17l** (Fig. 2). We have found that a simple metric that takes into  
22  
23 consideration both  $EC_{50}$  and  $R_{max}$  values, while also accounting for bimodal responses, is an  
24  
25 arithmetic sum of responses at each concentration tested ( $\Sigma[R_{conc.1} + R_{conc.2} \dots + R_{conc.n}]$ ). When  
26  
27 the activity profiles of these compounds were analyzed using this method, a clear demarcation of  
28  
29 TLR8-active and TLR7/TLR8 dual-active compounds became apparent (Fig. 2C), which greatly  
30  
31 facilitated the down-selection of compounds for evaluation in secondary screens.  
32  
33  
34  
35  
36  
37

38 Key active compounds were screened for cytokine and chemokine induction in human  
39  
40 peripheral blood mononuclear cells (PBMCs) using a multiplexed immunoassay platform. TLR8  
41  
42 agonists upregulate the production of proinflammatory cytokines such as TNF- $\alpha$ , IL-1 $\beta$ , IL-8, as  
43  
44 well as a number of chemokines; in addition, TLR8 agonists are particularly potent in inducing  
45  
46 the Th1-biasing cytokines IFN- $\gamma$  and IL-12.<sup>40-45</sup> In contrast, TLR7 agonists, as mentioned earlier,  
47  
48 induce Type I interferons, a pattern that is clearly apparent in interferon/cytokine secretion  
49  
50 patterns induced by the pyrimidine diamines (Fig. 3). TLR8-dominant compounds such as **17j**,  
51  
52  
53 **17l** elicit TNF- $\alpha$ , IL-12p40, and IFN- $\gamma$ , whereas the TLR7-dominant analogue, **17a**, potently  
54  
55  
56  
57  
58  
59  
60

induces IFN- $\alpha$ , but not IFN- $\gamma$  (Fig. 3). It was gratifying to observe that **17h**, which is equipotent at both TLR7 and TLR8 elicits a balanced IFN- $\alpha$ /IFN- $\gamma$ /TNF- $\alpha$ /IL-12 responses (Fig. 3).

While multiplexed immunoassay platforms have proven useful in profiling innate immune-active compounds, there are numerous limitations: the 96-well format and significant per-kit cost precludes its use in large- or high-throughput screens; the dynamic range is small, and a range-finding experiment for each compound would prove prohibitively expensive, and the small dynamic range is also a consequence of significant prozone effects<sup>67, 68</sup> which further limit throughput in these assays. We have, therefore, long desired an alternate secondary screen platform that would permit the rapid and comprehensive evaluation of large numbers of compounds. Given that Th1-biased responses (as well as plasmacytoid versus myeloid dendritic cell responses; discussed below) can largely be inferred from IFN- $\alpha$ /IFN- $\gamma$ /TNF- $\alpha$  response patterns, we have developed a liquid-handler assisted, 384-well plate-based, high-throughput scalable assay capable of measuring these analytes in *ex vivo* human whole blood models. In this alternate platform, analyte detection is performed using cytokine reporter cell lines rather than with conventional immunoassays (described in detail in the Experimental Section), which permitted a detailed evaluation of the induction profiles key cytokines of all active compounds reported, in quadruplicates (Figs. 4 and S3). Compound **17u**, was confirmed to be the most potent dual TLR7/TLR8 agonist (Figs. 2c and 4). The data derived from the cytokine reporter assays are, in general, concordant with EC<sub>50</sub> values derived from TLR-specific primary screens. Furthermore, a clear dependence of IFN- $\alpha$ / $\beta$  induction on TLR7 activity ( $P = 0.01$ ) and the dependence of IFN- $\gamma$ /TNF- $\alpha$ /IL-1 $\beta$  on TLR8 engagement ( $P = 0.005$  and  $<0.0001$ , respectively) was observed (Fig. 5). The superior sensitivity and dynamic range of the functional cytokine reporter assay (Figs. 4, 5) allows for a clear discrimination in small differences in potencies. It

should be noted, however, that direct correlations between cytokine reporter assay readouts and conventional, analyte-specific immunoassays are not feasible because cytokine reporter responses are functional in nature and are inherently ‘multiplexed’, i.e., the TNF- $\alpha$ /IL-1 $\beta$  cells respond to both TNF- $\alpha$  and IL-1 $\beta$  signals, and the IFN- $\alpha$ / $\beta$  cells respond to virtually all 13 IFN- $\alpha$  proteins as well as IFN- $\beta$ 1, IFN- $\beta$ 2 and, partially, to IFN- $\omega$ 1 (data not shown). We hope that this assay platform will prove useful to investigators focusing on innate immunity and vaccine adjuvant discovery.

Mention was made earlier of predominant expression of TLR7 in pDCs and of TLR8 in cDCs, and of the impact of pDC-derived Type I interferons (IFN- $\alpha$ / $\beta$ ) on Th1-polarized adaptive immune responses,<sup>56,57</sup> and the influence of cDC-derived TNF- $\alpha$ , IL-12, and IL-18 in augmenting Th1 responses.<sup>58, 60-62</sup> Given that we continue to find that dual TLR7/8 agonists perform better than either pure TLR7 or pure TLR8 agonists (manuscript in preparation), it was of particular interest to examine functional responses in these subsets of professional antigen-presenting cells. Dose-response profiles of CD80 expression in human peripheral blood dendritic cell populations (pDCs, CD141<sup>+</sup> cDCs, and CD1c<sup>+</sup> cDCs)<sup>69-71</sup> were evaluated. pDCs were defined as Live, Lin<sup>-</sup>, CD123<sup>+</sup>, CD303<sup>+</sup>, CD304<sup>+</sup>, HLA-DR<sup>+</sup>. CD141<sup>+</sup> cDCs were defined as Live, Lin<sup>-</sup>, CD1c<sup>-</sup>, CD141<sup>+</sup>, HLA-DR<sup>+</sup>. CD1c<sup>+</sup> cDC were defined as Live, Lin<sup>-</sup>, CD141<sup>-</sup>, CD1c<sup>+</sup>, CD11c<sup>+</sup>, HLA-DR<sup>+</sup> (Fig. 6). In these experiments, we included as comparators pure TLR7 (**1a**),<sup>32</sup> pure TLR8 (**1m**),<sup>41</sup> and dual TLR7/TLR8 (**1c**)<sup>65</sup> agonists. The results, shown in Fig. 7, are instructive: significant activation by the pure TLR8 agonist **1m** is observed only in the CD1c<sup>+</sup> cDC subset, whereas the dual-active TLR7/8 comparator **1c**, and the most potent analogue of this series, **17u** activate all DC subsets (Fig. 7).

## Conclusions

In conclusion, a systematic exploration of the pyrimidine-2,4-diamine chemotype has yielded high-potency TLR8-specific and dual TLR7/TLR8-active compounds. The novel dual TLR7/TLR8-active lead compound, **17u**, is on par with the most potent dual TLR7/TLR8 agonist that we have characterized thus far. The synthetic route to Compound **17u** is far more straightforward than it is to access highly functionalized imidazoquinolines. A detailed examination of activation in human peripheral blood dendritic cell subsets indicate that dual TLR7/8 agonists activate multiple dendritic cell subsets, including pDCs, CD141<sup>+</sup> cDCs, and CD1c<sup>+</sup> cDCs. The immunological consequences of enhanced antigen presentation by dual TLR7/8 agonists on adjuvant activity will be the focus of a future communication.

## Experimental Section

**Chemistry.** All of the solvents and reagents used were obtained commercially and used as such unless noted otherwise. Moisture- or air-sensitive reactions were conducted under nitrogen atmosphere in oven-dried (120 °C) glass apparatus. Solvents were removed under reduced pressure using standard rotary evaporators. Flash column chromatography was carried out using RediSep Rf 'Gold' high performance silica columns on CombiFlash R<sub>f</sub> instruments unless otherwise mentioned; thin-layer chromatography was carried out on silica gel CCM pre-coated aluminum sheets. Purity for all final compounds was confirmed to be greater than 98% by LC-MS using a Zorbax Eclipse Plus 4.6 mm x 150 mm, 5 µm analytical reverse phase C<sub>18</sub> column with H<sub>2</sub>O-CH<sub>3</sub>CN and H<sub>2</sub>O-MeOH gradients and an Agilent 6520 ESI-QTOF Accurate Mass spectrometer (mass accuracy of 5 ppm) operating in the positive ion acquisition mode. Compound **14a** was synthesized as published by us earlier.<sup>39</sup>

**N<sup>4</sup>-Butyl-5,6-dimethylpyrimidine-2,4-diamine (3).** To a solution of compound **2** (31.5 mg, 0.2 mmol) in MeOH (2 mL), were added Et<sub>3</sub>N (56 µL, 0.4 mmol) and butylamine (39.5 µL, 0.4 mmol). The reaction mixture was stirred for 12 h at 70 °C. The reaction mixture was cooled to room temperature and the solvent was removed under reduced pressure, and the crude material was purified by flash chromatography (10% MeOH/CH<sub>2</sub>Cl<sub>2</sub>) to afford the compound **3** as a white solid (30 mg, 77%). <sup>1</sup>H NMR (500 MHz, CDCl<sub>3</sub>) δ 4.59 (s, 2H), 4.36 (s, 1H), 3.43 – 3.35 (m, 2H), 2.20 (s, 3H), 1.87 (s, 3H), 1.60 – 1.51 (m, 2H), 1.44 – 1.32 (m, 2H), 0.93 (t, *J* = 7.4 Hz, 3H). <sup>13</sup>C NMR (126 MHz, CDCl<sub>3</sub>) δ 161.9, 161.1, 160.6, 100.7, 40.9, 32.0, 21.7, 20.3, 14.0, 10.9. MS (ESI-QTOF) for C<sub>10</sub>H<sub>18</sub>N<sub>4</sub> [M + H]<sup>+</sup> calculated 195.1604, found 195.1597.

***N*<sup>4</sup>-Butyl-5-ethyl-6-methylpyrimidine-2,4-diamine (6a).** A suspension of compound **4a** (153 mg, 1 mmol) in phosphorus(V) oxychloride (3 mL) was placed in a pressure vessel. The reaction mixture was stirred for 3 h at 85 °C. The reaction mixture was cooled to room temperature and the solvent was removed under reduced pressure. The reaction mixture was diluted with water and extracted with EtOAc (3 x 30 mL). The combined organic layer was dried over Na<sub>2</sub>SO<sub>4</sub> and concentrated under reduced pressure, and the crude material was purified by flash chromatography (60% EtOAc/hexanes) to afford the compound **5a** as a white solid (95 mg, 55%). MS (ESI-QTOF) for C<sub>7</sub>H<sub>10</sub>ClN<sub>3</sub> [M + H]<sup>+</sup> calculated 172.0636, found 172.0592. To a solution of **5a** (34.2 mg, 0.2 mmol) in MeOH (2 mL), was added Et<sub>3</sub>N (56 µL, 0.4 mmol) and butylamine (39.5 µL, 0.4 mmol). The reaction mixture was stirred for 12 h at 70 °C. The reaction mixture was cooled to room temperature and the solvent was removed under reduced pressure, and the crude material was purified by flash chromatography (10% MeOH/CH<sub>2</sub>Cl<sub>2</sub>) to afford the compound **6a** as a white solid (26 mg, 62%). <sup>1</sup>H NMR (500 MHz, CDCl<sub>3</sub>) δ 4.63 (s, 2H), 4.50 (s, 1H), 3.45 – 3.37 (m, 2H), 2.35 (q, *J* = 7.6 Hz, 2H), 2.22 (s, 3H), 1.62 – 1.52 (m, 2H), 1.45 – 1.34 (m, 2H), 1.06 (t, *J* = 7.6 Hz, 3H), 0.95 (t, *J* = 7.4 Hz, 3H). <sup>13</sup>C NMR (126 MHz, CDCl<sub>3</sub>) δ 161.4, 160.3, 160.2, 107.2, 40.9, 32.0, 20.9, 20.3, 18.8, 14.0, 12.8. MS (ESI-QTOF) for C<sub>11</sub>H<sub>20</sub>N<sub>4</sub> [M + H]<sup>+</sup> calculated 209.1761, found 209.1757.

Compound **6b** was synthesized similarly as compound **6a**.

***N*<sup>4</sup>,5-Dibutyl-6-methylpyrimidine-2,4-diamine (6b).**



Intermediate compound **5b**. Compound **4b** was used as reagent. White solid (88 mg, 44%). MS (ESI-QTOF) for  $C_9H_{14}ClN_3$   $[M + H]^+$  calculated 200.0949, found 200.0905.

Compound **6b**. White solid (30 mg, 63%).  $^1H$  NMR (500 MHz, MeOD)  $\delta$  3.37 (t,  $J = 7.2$  Hz, 2H), 2.37 (t,  $J = 6.5$  Hz, 2H), 2.15 (s, 3H), 1.62 – 1.52 (m, 2H), 1.43 – 1.32 (m, 6H), 0.99 – 0.92 (m, 6H).  $^{13}C$  NMR (126 MHz, MeOD)  $\delta$  163.0, 161.9, 160.8, 107.1, 41.5, 32.8, 32.0, 25.7, 23.7, 21.2, 20.6, 14.4, 14.3. MS (ESI-QTOF) for  $C_{13}H_{24}N_4$   $[M + H]^+$  calculated 237.2074, found 237.2066.

***N*<sup>4</sup>-Butyl-6-methylpyrimidine-2,4-diamine (8)**. To a solution of compound **7** (574.4 mg, 4 mmol) in MeOH (15 mL), was added Et<sub>3</sub>N (1120  $\mu$ L, 8 mmol) and butylamine (790.6  $\mu$ L, 8 mmol). The reaction mixture was stirred for 12 h at 70 °C. The reaction mixture was cooled to room temperature and the solvent was removed under reduced pressure, and the crude material was purified by flash chromatography (10% MeOH/CH<sub>2</sub>Cl<sub>2</sub>) to afford the compound **8** as a white solid (540 mg, 75%).  $^1H$  NMR (500 MHz, CDCl<sub>3</sub>)  $\delta$  5.61 (s, 1H), 4.81 (s, 2H), 4.72 (s, 1H), 3.24 – 3.16 (m, 2H), 2.18 (s, 3H), 1.58 – 1.49 (m, 2H), 1.43 – 1.31 (m, 2H), 0.92 (t,  $J = 7.3$  Hz, 3H).  $^{13}C$  NMR (126 MHz, CDCl<sub>3</sub>)  $\delta$  166.3, 164.1, 162.8, 93.1, 41.2, 31.7, 24.0, 20.2, 13.9. MS (ESI-QTOF) for  $C_9H_{16}N_4$   $[M + H]^+$  calculated 181.1448, found 181.1442.

***N*<sup>4</sup>-Butyl-5-iodo-6-methylpyrimidine-2,4-diamine (9)**. To a solution of compound **8** (360 mg, 2 mmol) in anhydrous DMF (5 mL) was added NIS (450 mg, 2 mmol), and the reaction mixture was stirred for 12 h. The reaction mixture was diluted with water and extracted with EtOAc (3 x 50 mL). The combined organic layer was dried over Na<sub>2</sub>SO<sub>4</sub>, concentrated under reduced pressure, and the crude material was purified by flash chromatography (70% EtOAc/hexanes) to

obtain the compound **9** as a white solid (520 mg, 85 %).  $^1\text{H}$  NMR (500 MHz,  $\text{CDCl}_3$ )  $\delta$  5.24 (s, 1H), 4.76 (s, 2H), 3.42 – 3.34 (m, 2H), 2.40 (s, 3H), 1.63 – 1.53 (m, 2H), 1.44 – 1.34 (m, 2H), 0.95 (t,  $J$  = 7.4 Hz, 3H).  $^{13}\text{C}$  NMR (126 MHz,  $\text{CDCl}_3$ )  $\delta$  166.5, 162.2, 161.0, 68.5, 41.6, 31.6, 28.8, 20.3, 14.0. MS (ESI-QTOF) for  $\text{C}_9\text{H}_{15}\text{IN}_4$   $[\text{M} + \text{H}]^+$  calculated 307.0414, found 307.0408.

***N*<sup>4</sup>-Butyl-6-methyl-5-pentylpyrimidine-2,4-diamine (11a)**. To a solution of compound **9** (61.2 mg, 0.2 mmol) in 2:1 mixture of DMF (2 mL) and DIPEA (1 mL) were added  $\text{Pd}(\text{PPh}_3)_4$  (23.1 mg, 0.02 mmol) and CuI (7.6 mg, 0.04 mmol). The reaction mixture was degassed with dry nitrogen for 5 min, then 1-pentyne (39.4  $\mu\text{L}$ , 0.4 mmol) was added. The resulting reaction mixture was stirred for 12 h under nitrogen atmosphere. After completion of the reaction, the mixture was diluted with water and extracted with ethylacetate (3 x 20 mL). The combined organic layer was dried over  $\text{Na}_2\text{SO}_4$  and concentrated under reduced pressure, the crude material was purified by flash chromatography (90% EtOAc/hexanes) to obtain the compound **10a** as yellow oil (38 mg, 77%).  $^1\text{H}$  NMR (500 MHz,  $\text{CDCl}_3$ )  $\delta$  5.36 (s, 1H), 4.76 (s, 2H), 3.44 – 3.36 (m, 2H), 2.46 (t,  $J$  = 6.9 Hz, 2H), 2.31 (s, 3H), 1.69 – 1.52 (m, 4H), 1.45 – 1.34 (m, 2H), 1.05 (t,  $J$  = 7.4 Hz, 3H), 0.95 (t,  $J$  = 7.3 Hz, 3H).  $^{13}\text{C}$  NMR (126 MHz,  $\text{CDCl}_3$ )  $\delta$  166.7, 163.1, 160.5, 99.7, 92.1, 74.0, 40.5, 31.9, 22.8, 22.6, 22.0, 20.2, 14.0, 13.7. MS (ESI-QTOF) for  $\text{C}_{14}\text{H}_{22}\text{N}_4$   $[\text{M} + \text{H}]^+$  calculated 247.1917, found 247.1939. To a solution of compound **10a** (24.6 mg, 0.1 mmol) in anhydrous EtOAc (10 mL) was added a catalytic amount of Pd/C, and the reaction mixture was subjected to hydrogenation at 50 psi for 5 h. The reaction mixture was filtered, and the filtrate was concentrated under reduced pressure. The crude material was purified by flash chromatography (10% MeOH/ $\text{CH}_2\text{Cl}_2$ ) to obtain the compound **11a** as a pale oil (20 mg, 80%).  $^1\text{H}$  NMR (500 MHz, MeOD)  $\delta$  3.38 (t,  $J$  = 7.2 Hz, 2H), 2.37 (t,  $J$  = 7.6 Hz, 2H),

2.16 (s, 3H), 1.62 – 1.52 (m, 2H), 1.46 – 1.32 (m, 8H), 0.98 – 0.90 (m, 6H).  $^{13}\text{C}$  NMR (126 MHz, MeOD)  $\delta$  163.1, 161.5, 160.2, 107.2, 41.5, 32.8, 32.7, 29.4, 25.8, 23.8, 21.2, 20.4, 14.4, 14.3. MS (ESI-QTOF) for  $\text{C}_{14}\text{H}_{26}\text{N}_4$   $[\text{M} + \text{H}]^+$  calculated 251.2230, found 251.2228.

Compounds **11b-d** were synthesized similarly as compound **11a**.

**4-(2-Amino-4-(butylamino)-6-methylpyrimidin-5-yl)butan-1-ol (11b).**

Intermediate compound **10b**. But-3-yn-1-ol was used as reagent. Yellow solid (40 mg, 80%). MS (ESI-QTOF) for  $\text{C}_{13}\text{H}_{20}\text{N}_4\text{O}$   $[\text{M} + \text{H}]^+$  calculated 249.1710, found 249.1689.

Compound **11b**. White solid (20 mg, 79%).  $^1\text{H}$  NMR (500 MHz, MeOD)  $\delta$  3.60 (t,  $J = 6.4$  Hz, 2H), 3.38 (t,  $J = 7.2$  Hz, 2H), 2.41 (t,  $J = 8.0$  Hz, 2H), 2.17 (s, 3H), 1.63 – 1.55 (m, 4H), 1.52 – 1.46 (m, 2H), 1.42 – 1.34 (m, 2H), 0.95 (t,  $J = 7.4$  Hz, 3H).  $^{13}\text{C}$  NMR (126 MHz, MeOD)  $\delta$  163.1, 161.7, 160.4, 107.1, 62.7, 41.6, 32.9, 32.7, 26.0, 25.5, 21.2, 20.4, 14.3. MS (ESI-QTOF) for  $\text{C}_{13}\text{H}_{24}\text{N}_4\text{O}$   $[\text{M} + \text{H}]^+$  calculated 253.2023, found 253.2011.

**4-(2-Amino-4-(butylamino)-6-methylpyrimidin-5-yl)-2-methylbutan-2-ol (11c).**

Intermediate compound **10c**. 2-Methylbut-3-yn-2-ol was used as reagent. Yellow solid (42 mg, 80%). MS (ESI-QTOF) for  $\text{C}_{14}\text{H}_{22}\text{N}_4\text{O}$   $[\text{M} + \text{H}]^+$  calculated 263.1866, found 263.1868.

Compound **11c**. White solid (20 mg, 75%).  $^1\text{H}$  NMR (500 MHz, MeOD)  $\delta$  3.38 (t,  $J = 7.2$  Hz, 2H), 2.47 – 2.40 (m, 2H), 2.16 (s, 3H), 1.61 – 1.55 (m, 2H), 1.53 – 1.49 (m, 2H), 1.44 – 1.37 (m, 2H), 1.26 (s, 6H), 0.96 (t,  $J = 7.4$  Hz, 3H).  $^{13}\text{C}$  NMR (126 MHz, MeOD)  $\delta$  162.9, 161.8, 160.3, 107.1, 71.2, 42.4, 41.6, 32.6, 29.3, 21.3, 20.5, 20.3, 14.2. MS (ESI-QTOF) for  $\text{C}_{14}\text{H}_{26}\text{N}_4\text{O}$   $[\text{M} + \text{H}]^+$  calculated 267.2179, found 267.2177.

**5-(2-Amino-4-(butylamino)-6-methylpyrimidin-5-yl)-2-methylpentan-2-ol (11d).**

Intermediate compound **10d**. 2-Methylpent-4-yn-2-ol was used as reagent. Yellow oil (46 mg, 83%). MS (ESI-QTOF) for  $C_{15}H_{24}N_4O$   $[M + H]^+$  calculated 277.2023, found 277.2029.

Compound **11d**. White solid (22 mg, 78%).  $^1H$  NMR (500 MHz, MeOD)  $\delta$  3.38 (t,  $J = 7.1$  Hz, 2H), 2.42 – 2.36 (m, 2H), 2.16 (s, 3H), 1.61 – 1.54 (m, 2H), 1.53 – 1.49 (m, 4H), 1.42 – 1.34 (m, 2H), 1.17 (s, 6H), 0.95 (t,  $J = 7.4$  Hz, 3H).  $^{13}C$  NMR (126 MHz, MeOD)  $\delta$  163.1, 161.8, 160.8, 107.0, 71.4, 43.9, 41.5, 32.8, 29.3, 26.3, 24.3, 21.2, 20.6, 14.3. MS (ESI-QTOF) for  $C_{15}H_{28}N_4O$   $[M + H]^+$  calculated 281.2336, found 281.2336.

***N*<sup>4</sup>-Butyl-5-ethynyl-6-methylpyrimidine-2,4-diamine (13)**. To a solution of compound **9** (92 mg, 0.3 mmol) in 2:1 mixture of DMF (3 mL) and DIPEA (1.5 mL) were added  $Pd(PPh_3)_4$  (34.6 mg, 0.03 mmol) and CuI (11.4 mg, 0.06 mmol). The reaction mixture was degassed with dry nitrogen for 5 min, then ethynyltrimethylsilane (83  $\mu$ L, 0.6 mmol) was added. The resulting reaction mixture was stirred for 12 h under nitrogen atmosphere. After completion of the reaction, the mixture was diluted with water and extracted with ethylacetate (3 x 30 mL). The combined organic layer was dried over  $Na_2SO_4$  and concentrated under reduced pressure, the crude material was purified by flash chromatography (50% EtOAc/hexanes) to obtain the compound **12** as white solid (63 mg, 76%).  $^1H$  NMR (500 MHz,  $CDCl_3$ )  $\delta$  5.39 (s, 1H), 4.91 (s, 2H), 3.45 – 3.37 (m, 2H), 2.33 (s, 3H), 1.62 – 1.52 (m, 2H), 1.46 – 1.35 (m, 2H), 0.96 (t,  $J = 7.4$  Hz, 3H), 0.25 (s, 9H).  $^{13}C$  NMR (126 MHz,  $CDCl_3$ )  $\delta$  167.9, 163.3, 160.8, 104.4, 99.3, 91.4, 40.5, 31.8, 22.9, 20.2, 14.0, 0.3. MS (ESI-QTOF) for  $C_{14}H_{24}N_4Si$   $[M + H]^+$  calculated 277.1843, found 277.1816. To a solution of **12** (27.6 mg, 0.1 mmol) in MeOH (2 mL) was added  $K_2CO_3$

(13.8 g, 0.1 mmol). The reaction mixture was stirred for 3 h. After completion of the reaction, the mixture was diluted with water and extracted with ethylacetate (3 x 20 mL). The combined organic layer was dried over Na<sub>2</sub>SO<sub>4</sub> and concentrated under reduced pressure, the crude material was purified by flash chromatography (50% EtOAc/hexanes) to obtain the compound **13** as yellow oil (14 mg, 69%). <sup>1</sup>H NMR (500 MHz, CDCl<sub>3</sub>) δ 5.39 (s, 1H), 4.92 (s, 2H), 3.61 (s, 1H), 3.45 – 3.37 (m, 2H), 2.34 (s, 3H), 1.62 – 1.52 (m, 2H), 1.45 – 1.33 (m, 2H), 0.95 (t, *J* = 7.4 Hz, 3H). <sup>13</sup>C NMR (126 MHz, CDCl<sub>3</sub>) δ 168.3, 163.5, 161.0, 90.1, 87.0, 78.1, 40.6, 31.8, 22.8, 20.2, 14.0. MS (ESI-QTOF) for C<sub>11</sub>H<sub>16</sub>N<sub>4</sub> [M + H]<sup>+</sup> calculated 205.1448, found 205.1445.

***N*<sup>4</sup>-Butyl-6-methyl-5-phenethylpyrimidine-2,4-diamine (14b)**. To a solution of compound **9** (61.2 mg, 0.2 mmol), *trans*-2-phenylvinylboronic acid (44.4 mg, 0.3 mmol) and K<sub>2</sub>CO<sub>3</sub> (83 mg, 0.6 mmol) in 4:1 mixture of 1,4-dioxane (3 mL) and water (0.75 mL) was added Pd(dppf)Cl<sub>2</sub> (11 mg, 0.015 mmol). The reaction mixture was degassed with dry nitrogen for 5 min, then stirred for 12 h at 85 °C under nitrogen atmosphere. The reaction mixture was diluted with water and extracted with EtOAc (3 x 20 mL). The combined organic layer was dried over Na<sub>2</sub>SO<sub>4</sub>, concentrated under reduced pressure, and the crude material was purified by flash chromatography (10% MeOH/CH<sub>2</sub>Cl<sub>2</sub>) to obtain the compound **15** as a yellow oil (44 mg, 78%). MS (ESI-QTOF) for C<sub>17</sub>H<sub>22</sub>N<sub>4</sub> [M + H]<sup>+</sup> calculated 283.1917, found 283.1890. To a solution of compound **15** (28.2 mg, 0.1 mmol) in anhydrous EtOAc (10 mL) was added a catalytic amount of Pd/C, and the reaction mixture was subjected to hydrogenation at 50 psi for 5 h. The reaction mixture was filtered, and the filtrate was concentrated under reduced pressure. The crude material was purified by flash chromatography (10% MeOH/CH<sub>2</sub>Cl<sub>2</sub>) to obtain the compound **14b** as a white solid (20 mg, 70%). <sup>1</sup>H NMR (500 MHz, MeOD) δ 7.24 – 7.21 (m, 2H), 7.17 –

7.14 (m, 1H), 7.11 (d,  $J = 7.4$  Hz, 2H), 3.35 (t,  $J = 7.2$  Hz, 2H), 2.77 – 2.65 (m, 4H), 1.84 (s, 3H), 1.60 – 1.50 (m, 2H), 1.44 – 1.32 (m, 2H), 0.96 (t,  $J = 7.4$  Hz, 3H).  $^{13}\text{C}$  NMR (126 MHz, MeOD)  $\delta$  163.1, 161.9, 161.6, 142.8, 129.9, 129.3, 127.0, 105.8, 41.6, 35.4, 32.8, 28.0, 21.3, 20.4, 14.3. MS (ESI-QTOF) for  $\text{C}_{17}\text{H}_{24}\text{N}_4$   $[\text{M} + \text{H}]^+$  calculated 285.2074, found 285.2065.

Compounds **17a-p** were synthesized similarly as compound **11a**.

***N*<sup>4</sup>-Butyl-6-methyl-5-(3-phenylpropyl)pyrimidine-2,4-diamine (17a).**

Intermediate compound **16a**. Prop-2-yn-1-ylbenzene was used as reagent. Yellow solid (46 mg, 78%).  $^1\text{H}$  NMR (500 MHz, MeOD)  $\delta$  7.42 – 7.40 (m, 2H), 7.35 – 7.31 (m, 2H), 7.25 – 7.22 (m, 1H), 3.91 (s, 2H), 3.39 (t,  $J = 7.1$  Hz, 2H), 2.27 (s, 3H), 1.57 – 1.51 (m, 2H), 1.39 – 1.31 (m, 2H), 0.94 (t,  $J = 7.4$  Hz, 3H).  $^{13}\text{C}$  NMR (126 MHz, MeOD)  $\delta$  166.8, 164.3, 162.1, 138.7, 129.6, 128.9, 127.7, 98.6, 92.3, 76.1, 41.3, 32.8, 26.7, 22.3, 21.1, 14.2. MS (ESI-QTOF) for  $\text{C}_{18}\text{H}_{22}\text{N}_4$   $[\text{M} + \text{H}]^+$  calculated 295.1917, found 295.1941.

Compound **17a**. Pale oil (23 mg, 77%).  $^1\text{H}$  NMR (500 MHz, MeOD)  $\delta$  7.29 – 7.25 (m, 2H), 7.22 – 7.15 (m, 3H), 3.36 (t,  $J = 7.1$  Hz, 2H), 2.68 (t,  $J = 7.5$  Hz, 2H), 2.38 (t,  $J = 8.0$  Hz, 2H), 2.07 (s, 3H), 1.77 – 1.67 (m, 2H), 1.58 – 1.49 (m, 2H), 1.41 – 1.29 (m, 2H), 0.95 (t,  $J = 7.4$  Hz, 3H).  $^{13}\text{C}$  NMR (126 MHz, MeOD)  $\delta$  163.0, 161.5, 160.1, 143.5, 129.5, 129.4, 126.9, 106.8, 41.6, 36.5, 32.7, 31.4, 25.2, 21.2, 20.2, 14.3. MS (ESI-QTOF) for  $\text{C}_{18}\text{H}_{26}\text{N}_4$   $[\text{M} + \text{H}]^+$  calculated 299.2230, found 299.2253.

***N*<sup>4</sup>-Butyl-6-methyl-5-(4-phenylbutyl)pyrimidine-2,4-diamine (17b).**

Intermediate compound **16b**. But-3-yn-1-ylbenzene was used as reagent. Yellow solid (48 mg, 78%). MS (ESI-QTOF) for  $C_{19}H_{24}N_4$   $[M + H]^+$  calculated 309.2074, found 309.2013.

Compound **17b**. Pale oil (25 mg, 80%).  $^1H$  NMR (500 MHz, MeOD)  $\delta$  7.26 – 7.23 (m, 2H), 7.18 – 7.12 (m, 3H), 3.37 (t,  $J = 7.2$  Hz, 2H), 2.64 (t,  $J = 7.6$  Hz, 2H), 2.40 (t,  $J = 7.9$  Hz, 2H), 2.14 (s, 3H), 1.73 – 1.67 (m, 2H), 1.56 – 1.50 (m, 2H), 1.47 – 1.41 (m, 2H), 1.37 – 1.31 (m, 2H), 0.93 (t,  $J = 7.4$  Hz, 3H).  $^{13}C$  NMR (126 MHz, MeOD)  $\delta$  163.1, 160.9, 159.0, 143.6, 129.4, 129.3, 126.7, 107.2, 41.6, 36.8, 32.7, 32.2, 29.1, 25.5, 21.2, 20.0, 14.3. MS (ESI-QTOF) for  $C_{19}H_{28}N_4$   $[M + H]^+$  calculated 313.2387, found 313.2356.

***N*<sup>4</sup>-Butyl-6-methyl-5-(5-phenylpentyl)pyrimidine-2,4-diamine (17c).**

Intermediate compound **16c**. Pent-4-yn-1-ylbenzene was used as reagent. Yellow oil (50 mg, 78%). MS (ESI-QTOF) for  $C_{20}H_{26}N_4$   $[M + H]^+$  calculated 323.2230, found 323.2261.

Compound **17c**. Pale oil (25 mg, 76%).  $^1H$  NMR (500 MHz, MeOD)  $\delta$  7.25 – 7.21 (m, 2H), 7.15 – 7.11 (m, 3H), 3.38 (t,  $J = 7.2$  Hz, 2H), 2.61 (t,  $J = 7.6$  Hz, 2H), 2.37 (t,  $J = 7.5$  Hz, 2H), 2.14 (s, 3H), 1.67 – 1.61 (m, 2H), 1.59 – 1.53 (m, 2H), 1.47 – 1.33 (m, 6H), 0.95 (t,  $J = 7.4$  Hz, 3H).  $^{13}C$  NMR (126 MHz, MeOD)  $\delta$  163.1, 161.2, 159.6, 143.8, 129.4, 129.3, 126.7, 107.2, 41.6, 36.8, 32.8, 32.7, 30.0, 29.5, 25.7, 21.2, 20.2, 14.3. MS (ESI-QTOF) for  $C_{20}H_{30}N_4$   $[M + H]^+$  calculated 327.2543, found 327.2581.

***N*<sup>4</sup>-Butyl-5-(3-cyclohexylpropyl)-6-methylpyrimidine-2,4-diamine (17d).**

Intermediate compound **16d**. Prop-2-yn-1-ylcyclohexane was used as reagent. Yellow solid (48 mg, 80%). MS (ESI-QTOF) for  $C_{18}H_{28}N_4$   $[M + H]^+$  calculated 301.2387, found 301.2384.

Compound **17d**. White solid (25 mg, 82%).  $^1\text{H}$  NMR (500 MHz, MeOD)  $\delta$  3.40 (t,  $J = 7.1$  Hz, 2H), 2.36 (t,  $J = 7.7$  Hz, 2H), 2.16 (s, 3H), 1.74 – 1.64 (m, 5H), 1.60 – 1.54 (m, 2H), 1.47 – 1.34 (m, 4H), 1.30 – 1.15 (m, 6H), 0.95 (t,  $J = 7.4$  Hz, 3H), 0.92 – 0.86 (m, 2H).  $^{13}\text{C}$  NMR (126 MHz, MeOD)  $\delta$  163.1, 161.0, 159.2, 107.4, 41.6, 39.1, 38.3, 34.6, 32.7, 27.8, 27.5, 26.9, 25.9, 21.2, 20.1, 14.3. MS (ESI-QTOF) for  $\text{C}_{18}\text{H}_{32}\text{N}_4$   $[\text{M} + \text{H}]^+$  calculated 305.2700, found 305.2711.

**5-(3-(1*H*-Pyrazol-1-yl)propyl)-*N*<sup>4</sup>-butyl-6-methylpyrimidine-2,4-diamine (17e).**

Intermediate compound **16e**. 1-(Prop-2-yn-1-yl)-1*H*-pyrazole was used as reagent. Pale yellow solid (40 mg, 70%). MS (ESI-QTOF) for  $\text{C}_{15}\text{H}_{20}\text{N}_6$   $[\text{M} + \text{H}]^+$  calculated 285.1822, found 285.1822.

Compound **17e**. White solid (16 mg, 55%).  $^1\text{H}$  NMR (500 MHz,  $\text{CDCl}_3$ )  $\delta$  7.56 (d,  $J = 1.4$  Hz, 1H), 7.42 (d,  $J = 2.2$  Hz, 1H), 6.31 – 6.30 (m, 1H), 5.83 (s, 1H), 4.59 (s, 2H), 4.16 (t,  $J = 5.8$  Hz, 2H), 3.41 – 3.37 (m, 2H), 2.34 (t,  $J = 7.7$  Hz, 2H), 2.19 (s, 3H), 2.06 – 2.00 (m, 2H), 1.62 – 1.56 (m, 2H), 1.42 – 1.35 (m, 2H), 0.95 (t,  $J = 7.3$  Hz, 3H).  $^{13}\text{C}$  NMR (126 MHz,  $\text{CDCl}_3$ )  $\delta$  162.0, 160.7, 160.6, 139.5, 130.1, 105.7, 104.8, 50.8, 41.0, 31.7, 28.2, 22.6, 21.1, 20.4, 14.1. MS (ESI-QTOF) for  $\text{C}_{15}\text{H}_{24}\text{N}_6$   $[\text{M} + \text{H}]^+$  calculated 289.2135, found 289.2138.

**5-(3-(1*H*-1,2,4-Triazol-1-yl)propyl)-*N*<sup>4</sup>-butyl-6-methylpyrimidine-2,4-diamine (17f).**

Intermediate compound **16f**. 1-(Prop-2-yn-1-yl)-1*H*-1,2,4-triazole was used as reagent. Yellow solid (45 mg, 79%). MS (ESI-QTOF) for  $\text{C}_{14}\text{H}_{19}\text{N}_7$   $[\text{M} + \text{H}]^+$  calculated 286.1775, found 286.1776.

Compound **17f**. White solid (22 mg, 76%).  $^1\text{H}$  NMR (500 MHz, MeOD)  $\delta$  8.47 (s, 1H), 8.03 (s, 1H), 4.30 (t,  $J = 6.8$  Hz, 2H), 3.39 (t,  $J = 7.1$  Hz, 2H), 2.40 (t,  $J = 7.9$  Hz, 2H), 2.10 (s, 3H), 2.03



– 1.96 (m, 2H), 1.62 – 1.56 (m, 2H), 1.42 – 1.34 (m, 2H), 0.96 (t,  $J = 7.4$  Hz, 3H).  $^{13}\text{C}$  NMR (126 MHz, MeOD)  $\delta$  163.1, 162.2, 161.4, 152.2, 145.2, 105.3, 49.9, 41.6, 32.7, 29.2, 23.0, 21.3, 20.4, 14.3. MS (ESI-QTOF) for  $\text{C}_{14}\text{H}_{23}\text{N}_7$   $[\text{M} + \text{H}]^+$  calculated 290.2088, found 290.2092.

**5-(3-(1*H*-Indol-1-yl)propyl)-*N*<sup>4</sup>-butyl-6-methylpyrimidine-2,4-diamine (17g).**

Intermediate compound **16g**. 1-(Prop-2-yn-1-yl)-1*H*-indole was used as reagent. Yellow oil (50 mg, 75%). MS (ESI-QTOF) for  $\text{C}_{20}\text{H}_{23}\text{N}_5$   $[\text{M} + \text{H}]^+$  calculated 334.2026, found 334.2027.

Compound **17g**. White solid (24 mg, 71%).  $^1\text{H}$  NMR (500 MHz,  $\text{CDCl}_3$ )  $\delta$  7.66 (d,  $J = 7.9$  Hz, 1H), 7.35 – 7.33 (m, 1H), 7.24 – 7.20 (m, 1H), 7.14 – 7.11 (m, 2H), 6.55 (d,  $J = 3.0$  Hz, 1H), 4.91 (s, 2H), 4.22 (t,  $J = 6.2$  Hz, 2H), 3.84 (s, 1H), 3.07 – 3.03 (m, 2H), 2.21 – 2.15 (m, 5H), 1.99 – 1.93 (m, 2H), 1.18 – 1.12 (m, 4H), 0.86 (t,  $J = 6.3$  Hz, 3H).  $^{13}\text{C}$  NMR (126 MHz,  $\text{CDCl}_3$ )  $\delta$  161.2, 159.6, 158.9, 135.9, 128.9, 128.0, 122.1, 121.5, 119.9, 109.5, 104.5, 101.8, 46.0, 40.9, 31.4, 28.5, 22.4, 20.3, 20.2, 14.0. MS (ESI-QTOF) for  $\text{C}_{20}\text{H}_{27}\text{N}_5$   $[\text{M} + \text{H}]^+$  calculated 338.2339, found 338.2341.

***N*<sup>4</sup>-Butyl-6-methyl-5-(3-(2-methyl-1*H*-benzo[*d*]imidazol-1-yl)propyl)pyrimidine-2,4-diamine (17h).**

Intermediate compound **16h**. 2-Methyl-1-(prop-2-yn-1-yl)-1*H*-benzo[*d*]imidazole was used as reagent. Pale yellow solid (50 mg, 72%). MS (ESI-QTOF) for  $\text{C}_{20}\text{H}_{24}\text{N}_6$   $[\text{M} + \text{H}]^+$  calculated 349.2135, found 349.2127.

Compound **17h**. White solid (28 mg, 79%).  $^1\text{H}$  NMR (500 MHz, MeOD)  $\delta$  7.56 (d,  $J = 8.7$  Hz, 1H), 7.44 (d,  $J = 7.5$  Hz, 1H), 7.26 – 7.20 (m, 2H), 4.28 (t,  $J = 7.3$  Hz, 2H), 3.35 (t,  $J = 7.2$  Hz, 2H), 2.60 (s, 3H), 2.42 (t,  $J = 8.2$  Hz, 2H), 2.00 (s, 3H), 1.96 – 1.86 (m, 2H), 1.56 – 1.46 (m,

2H), 1.38 – 1.27 (m, 2H), 0.92 (t,  $J = 7.4$  Hz, 3H).  $^{13}\text{C}$  NMR (126 MHz, MeOD)  $\delta$  162.9, 162.2, 161.4, 153.2, 142.9, 136.0, 123.5, 123.3, 119.0, 110.9, 105.3, 44.1, 41.5, 32.8, 29.3, 22.9, 21.2, 20.4, 14.3, 13.5. MS (ESI-QTOF) for  $\text{C}_{20}\text{H}_{28}\text{N}_6$   $[\text{M} + \text{H}]^+$  calculated 353.2448, found 353.2446.

**2-(3-(2-Amino-4-(butylamino)-6-methylpyrimidin-5-yl)propyl)isoindoline-1,3-dione (17i).**

Intermediate compound **16i**. 2-(Prop-2-yn-1-yl)isoindoline-1,3-dione was used as reagent. Yellow solid (52 mg, 72%). MS (ESI-QTOF) for  $\text{C}_{20}\text{H}_{21}\text{N}_5\text{O}_2$   $[\text{M} + \text{H}]^+$  calculated 364.1768, found 364.1786.

Compound **17i**. White solid (28 mg, 76%).  $^1\text{H}$  NMR (500 MHz, MeOD)  $\delta$  7.87 – 7.83 (m, 2H), 7.82 – 7.79 (m, 2H), 3.74 (t,  $J = 7.2$  Hz, 2H), 3.37 (t,  $J = 7.2$  Hz, 2H), 2.44 (t,  $J = 8.1$  Hz, 2H), 2.13 (s, 3H), 1.84 – 1.74 (m, 2H), 1.61 – 1.52 (m, 2H), 1.42 – 1.31 (m, 2H), 0.94 (t,  $J = 7.3$  Hz, 3H).  $^{13}\text{C}$  NMR (126 MHz, MeOD)  $\delta$  170.0, 163.0, 161.6, 160.2, 135.4, 133.4, 124.1, 106.0, 41.6, 38.7, 32.7, 28.2, 23.4, 21.2, 20.2, 14.3. MS (ESI-QTOF) for  $\text{C}_{20}\text{H}_{25}\text{N}_5\text{O}_2$   $[\text{M} + \text{H}]^+$  calculated 368.2081, found 368.2114.

***N*<sup>4</sup>-Butyl-5-(3-(isoindolin-2-yl)propyl)-6-methylpyrimidine-2,4-diamine (17j).**

Intermediate compound **16j**. 2-(Prop-2-yn-1-yl)isoindoline was used as reagent. Yellow solid (50 mg, 75%). MS (ESI-QTOF) for  $\text{C}_{20}\text{H}_{25}\text{N}_5$   $[\text{M} + \text{H}]^+$  calculated 336.2183, found 336.2192.

Compound **17j**. White solid (24 mg, 71%).  $^1\text{H}$  NMR (500 MHz, MeOD)  $\delta$  7.28 – 7.19 (m, 4H), 3.93 (s, 4H), 3.32 – 3.29 (m, 2H), 2.74 (t,  $J = 6.9$  Hz, 2H), 2.51 (t,  $J = 7.2$  Hz, 2H), 2.20 (s, 3H), 1.82 – 1.72 (m, 2H), 1.46 – 1.36 (m, 2H), 1.33 – 1.21 (m, 2H), 0.83 (t,  $J = 7.4$  Hz, 3H).  $^{13}\text{C}$  NMR (126 MHz, MeOD)  $\delta$  163.7, 162.1, 161.4, 140.8, 128.1, 123.3, 106.3, 59.8, 55.4, 41.9, 32.6, 28.4,

23.2, 21.3, 20.6, 14.2. MS (ESI-QTOF) for  $C_{20}H_{29}N_5$   $[M + H]^+$  calculated 340.2496, found 340.2506.

***N*<sup>4</sup>-Butyl-6-methyl-5-(3-(pyrrolidin-1-yl)propyl)pyrimidine-2,4-diamine (17k).**

Intermediate compound **16k**. 1-(Prop-2-yn-1-yl)pyrrolidine was used as reagent. Yellow solid (40 mg, 70%). MS (ESI-QTOF) for  $C_{16}H_{25}N_5$   $[M + H]^+$  calculated 288.2183, found 288.2163.

Compound **17k**. White solid (24 mg, 82%). <sup>1</sup>H NMR (500 MHz, MeOD)  $\delta$  3.38 (t,  $J$  = 7.2 Hz, 2H), 2.58 – 2.53 (m, 4H), 2.48 (t,  $J$  = 7.4 Hz, 2H), 2.43 (t,  $J$  = 7.5 Hz, 2H), 2.17 (s, 3H), 1.84 – 1.80 (m, 4H), 1.70 – 1.64 (m, 2H), 1.60 – 1.55 (m, 2H), 1.41 – 1.36 (m, 2H), 0.96 (t,  $J$  = 7.4 Hz, 3H). <sup>13</sup>C NMR (126 MHz, MeOD)  $\delta$  163.5, 161.9, 161.0, 106.4, 56.2, 54.9, 41.7, 32.9, 28.5, 24.2, 23.4, 21.3, 20.5, 14.3. MS (ESI-QTOF) for  $C_{16}H_{29}N_5$   $[M + H]^+$  calculated 292.2496, found 292.2494.

***N*<sup>4</sup>-Butyl-6-methyl-5-(3-(piperidin-1-yl)propyl)pyrimidine-2,4-diamine (17l).**

Intermediate compound **16l**. 1-(Prop-2-yn-1-yl)piperidine was used as reagent. Yellow solid (44 mg, 73%). <sup>1</sup>H NMR (500 MHz, CDCl<sub>3</sub>)  $\delta$  5.37 (s, 1H), 4.75 (s, 2H), 3.57 (s, 2H), 3.45 – 3.37 (m, 2H), 2.58 – 2.52 (m, 4H), 2.33 (s, 3H), 1.67 – 1.62 (m, 4H), 1.60 – 1.54 (m, 2H), 1.45 – 1.36 (m, 4H), 0.95 (t,  $J$  = 7.3 Hz, 3H). <sup>13</sup>C NMR (126 MHz, CDCl<sub>3</sub>)  $\delta$  167.3, 163.2, 160.7, 94.6, 91.4, 78.7, 53.5, 49.0, 40.6, 31.9, 26.1, 24.1, 23.1, 20.3, 14.0. MS (ESI-QTOF) for  $C_{17}H_{27}N_5$   $[M + H]^+$  calculated 302.2339, found 302.2346.

Compound **17l**. White solid (24 mg, 78%). <sup>1</sup>H NMR (500 MHz, MeOD)  $\delta$  3.39 (t,  $J$  = 7.2 Hz, 2H), 2.46 – 2.37 (m, 6H), 2.33 (t,  $J$  = 7.4 Hz, 2H), 2.16 (s, 3H), 1.67 – 1.55 (m, 8H), 1.51 – 1.47 (m, 2H), 1.42 – 1.36 (m, 2H), 0.95 (t,  $J$  = 7.4 Hz, 3H). <sup>13</sup>C NMR (126 MHz, MeOD)  $\delta$  163.4,

161.9, 161.0, 106.4, 59.1, 55.5, 41.5, 33.0, 26.7, 26.4, 25.3, 23.4, 21.3, 20.5, 14.3. MS (ESI-QTOF) for  $C_{17}H_{31}N_5$   $[M + H]^+$  calculated 306.2652, found 306.2664.

**5-(3-(Azepan-1-yl)propyl)-*N*<sup>4</sup>-butyl-6-methylpyrimidine-2,4-diamine (17m).**

Intermediate compound **16m**. 1-(Prop-2-yn-1-yl)azepane was used as reagent. Pale yellow solid (50 mg, 79%). MS (ESI-QTOF) for  $C_{18}H_{29}N_5$   $[M + H]^+$  calculated 316.2496, found 316.2495.

Compound **17m**. White solid (24 mg, 75%). <sup>1</sup>H NMR (500 MHz, CDCl<sub>3</sub>) δ 6.66 (s, 1H), 4.74 (s, 2H), 3.43 – 3.35 (m, 2H), 2.67 – 2.61 (m, 4H), 2.43 – 2.36 (m, 4H), 2.22 (s, 3H), 1.70 – 1.62 (m, 10H), 1.58 – 1.52 (m, 2H), 1.41 – 1.34 (m, 2H), 0.94 (t, *J* = 7.3 Hz, 3H). <sup>13</sup>C NMR (126 MHz, CDCl<sub>3</sub>) δ 163.0, 159.5, 158.8, 106.0, 55.1, 54.3, 41.1, 32.1, 27.3, 27.1, 26.4, 21.9, 20.4, 20.3, 14.1. MS (ESI-QTOF) for  $C_{18}H_{33}N_5$   $[M + H]^+$  calculated 320.2809, found 320.2818.

***N*<sup>4</sup>-Butyl-5-(3-(dimethylamino)propyl)-6-methylpyrimidine-2,4-diamine (17n).**

Intermediate compound **16n**. *N,N*-Dimethylprop-2-yn-1-amine was used as reagent. Yellow solid (38 mg, 73%). MS (ESI-QTOF) for  $C_{14}H_{23}N_5$   $[M + H]^+$  calculated 262.2026, found 262.2060.

Compound **17n**. White solid (20 mg, 75%). <sup>1</sup>H NMR (500 MHz, MeOD) δ 3.37 (t, *J* = 7.2 Hz, 2H), 2.41 (t, *J* = 7.5 Hz, 2H), 2.32 (t, *J* = 7.3 Hz, 2H), 2.24 (s, 6H), 2.16 (s, 3H), 1.67 – 1.53 (m, 4H), 1.45 – 1.33 (m, 2H), 0.96 (t, *J* = 7.4 Hz, 3H). <sup>13</sup>C NMR (126 MHz, MeOD) δ 163.4, 162.1, 161.2, 106.3, 59.4, 45.5, 41.6, 32.8, 27.3, 23.3, 21.3, 20.6, 14.3. MS (ESI-QTOF) for  $C_{14}H_{27}N_5$   $[M + H]^+$  calculated 266.2339, found 266.2370.

***N*<sup>4</sup>-Butyl-5-(3-(diethylamino)propyl)-6-methylpyrimidine-2,4-diamine (17o).**

Intermediate compound **16o**. *N,N*-Diethylprop-2-yn-1-amine was used as reagent. Yellow solid (44 mg, 76%). MS (ESI-QTOF) for  $C_{16}H_{27}N_5$   $[M + H]^+$  calculated 290.2339, found 290.2320.

Compound **17o**. White solid (20 mg, 68%).  $^1H$  NMR (500 MHz, MeOD)  $\delta$  3.41 (t,  $J = 7.2$  Hz, 2H), 2.67 (q,  $J = 7.2$  Hz, 4H), 2.60 (t,  $J = 7.1$  Hz, 2H), 2.42 (t,  $J = 7.7$  Hz, 2H), 2.19 (s, 3H), 1.66 – 1.55 (m, 4H), 1.42 – 1.34 (m, 2H), 1.09 (t,  $J = 7.2$  Hz, 6H), 0.96 (t,  $J = 7.4$  Hz, 3H).  $^{13}C$  NMR (126 MHz, MeOD)  $\delta$  163.3, 160.8, 158.7, 106.6, 52.8, 47.8, 41.7, 32.7, 26.0, 23.3, 21.3, 19.8, 14.3, 10.9. MS (ESI-QTOF) for  $C_{16}H_{31}N_5$   $[M + H]^+$  calculated 294.2652, found 294.2660.

***tert*-Butyl 4-(3-(2-amino-4-(butylamino)-6-methylpyrimidin-5-yl)propyl)piperazine-1-carboxylate (17p).**

Intermediate compound **16p**. *tert*-Butyl 4-(prop-2-yn-1-yl)piperazine-1-carboxylate was used as reagent. Yellow solid (60 mg, 75%). MS (ESI-QTOF) for  $C_{21}H_{34}N_6O_2$   $[M + H]^+$  calculated 403.2816, found 403.2780.

Compound **17p**. White solid (30 mg, 74%).  $^1H$  NMR (500 MHz, MeOD)  $\delta$  3.47 – 3.41 (m, 4H), 3.39 (t,  $J = 7.2$  Hz, 2H), 2.46 – 2.35 (m, 8H), 2.17 (s, 3H), 1.69 – 1.63 (m, 2H), 1.61 – 1.54 (m, 2H), 1.46 (s, 9H), 1.41 – 1.34 (m, 2H), 0.96 (t,  $J = 7.4$  Hz, 3H).  $^{13}C$  NMR (126 MHz, MeOD)  $\delta$  163.4, 161.9, 161.1, 156.4, 106.3, 81.3, 58.3, 54.0 (2C), 41.5, 33.0, 28.6, 26.3, 23.2, 21.3, 20.5, 14.3. MS (ESI-QTOF) for  $C_{21}H_{38}N_6O_2$   $[M + H]^+$  calculated 407.3129, found 407.3152.

***N*<sup>4</sup>-Butyl-6-methyl-5-(3-(piperazin-1-yl)propyl)pyrimidine-2,4-diamine trihydrochloride (17q).**

To a stirred solution of *N*-Boc protected compound **17p** (20.3 mg, 0.05 mmol) in 1,4-dioxane (1 mL) was added hydrogen chloride (1 mL, 4 M in dioxane), and the reaction mixture was stirred

for 3 h at room temperature. Excess solvent was removed under reduced pressure and the resulted residue was thoroughly washed with diethyl ether to obtain the desired compound **17q** as a white solid (16 mg, 77%).  $^1\text{H}$  NMR (500 MHz, MeOD)  $\delta$  3.92 – 3.82 (m, 2H), 3.75 – 3.64 (m, 4H), 3.56 – 3.47 (m, 4H), 3.41 (t,  $J$  = 7.5 Hz, 2H), 2.59 (t,  $J$  = 8.0 Hz, 2H), 2.34 (s, 3H), 1.99 – 1.91 (m, 2H), 1.70 – 1.60 (m, 2H), 1.44 – 1.33 (m, 2H), 0.96 (t,  $J$  = 7.4 Hz, 3H).  $^{13}\text{C}$  NMR (126 MHz, MeOD)  $\delta$  163.4, 155.8, 149.6, 106.9, 57.5, 49.8, 42.3, 42.0, 32.2, 23.5, 22.3, 21.2, 16.7, 14.2. MS (ESI-QTOF) for  $\text{C}_{16}\text{H}_{30}\text{N}_6$   $[\text{M} + \text{H}]^+$  calculated 307.2605, found 307.2632.

Compounds **17r-w** were synthesized similarly as compound **11a**.

***N*<sup>4</sup>-Butyl-6-methyl-5-(3-(4-methylpiperazin-1-yl)propyl)pyrimidine-2,4-diamine (17r).**

Intermediate compound **16r**. 1-Methyl-4-(prop-2-yn-1-yl)piperazine was used as reagent. Pale yellow solid (45 mg, 71%). MS (ESI-QTOF) for  $\text{C}_{17}\text{H}_{28}\text{N}_6$   $[\text{M} + \text{H}]^+$  calculated 317.2448, found 317.2445.

Compound **17r**. White solid (22 mg, 69%).  $^1\text{H}$  NMR (500 MHz,  $\text{CDCl}_3$ )  $\delta$  6.74 (s, 1H), 4.81 (s, 2H), 3.43 – 3.35 (m, 2H), 2.69 – 2.25 (m, 15H), 2.22 (s, 3H), 1.71 – 1.65 (m, 2H), 1.59 – 1.53 (m, 2H), 1.42 – 1.34 (m, 2H), 0.95 (t,  $J$  = 7.3 Hz, 3H).  $^{13}\text{C}$  NMR (126 MHz,  $\text{CDCl}_3$ )  $\delta$  162.9, 161.5, 160.6, 105.4, 55.6, 55.4, 52.9, 46.3, 40.7, 32.5, 25.5, 21.7, 21.2, 20.4, 14.1. MS (ESI-QTOF) for  $\text{C}_{17}\text{H}_{32}\text{N}_6$   $[\text{M} + \text{H}]^+$  calculated 321.2761, found 321.2795.

***N*<sup>4</sup>-Butyl-6-methyl-5-(3-(4-phenylpiperazin-1-yl)propyl)pyrimidine-2,4-diamine (17s).**

Intermediate compound **16s**. 1-Phenyl-4-(prop-2-yn-1-yl)piperazine was used as reagent. Pale yellow solid (57 mg, 75%). MS (ESI-QTOF) for  $C_{22}H_{30}N_6$   $[M + H]^+$  calculated 379.2605, found 379.2598.

Compound **17s**. Pale oil (26 mg, 68%).  $^1H$  NMR (500 MHz, MeOD)  $\delta$  7.25 – 7.22 (m, 2H), 6.99 – 6.96 (m, 2H), 6.86 – 6.83 (m, 1H), 3.44 (t,  $J = 7.2$  Hz, 2H), 3.20 (t,  $J = 5.0$  Hz, 4H), 2.65 (t,  $J = 5.0$  Hz, 4H), 2.50 – 2.41 (m, 4H), 2.22 (s, 3H), 1.76 – 1.66 (m, 2H), 1.64 – 1.54 (m, 2H), 1.42 – 1.34 (m, 2H), 0.95 (t,  $J = 7.4$  Hz, 3H).  $^{13}C$  NMR (126 MHz, MeOD)  $\delta$  163.6, 160.0, 157.4, 152.6, 130.1, 121.3, 117.5, 107.0, 58.1, 54.2, 50.4, 41.7, 32.8, 26.2, 23.0, 21.2, 19.3, 14.3. MS (ESI-QTOF) for  $C_{22}H_{34}N_6$   $[M + H]^+$  calculated 383.2918, found 383.2944.

***N*<sup>4</sup>-Butyl-6-methyl-5-(3-thiomorpholinopropyl)pyrimidine-2,4-diamine (17t).**

Intermediate compound **16t**. 4-(Prop-2-yn-1-yl)thiomorpholine was used as reagent. Pale yellow solid (40 mg, 63%). MS (ESI-QTOF) for  $C_{16}H_{25}N_5S$   $[M + H]^+$  calculated 320.1903, found 320.1880.

Compound **17t**. White solid (25 mg, 77%).  $^1H$  NMR (500 MHz, MeOD)  $\delta$  3.40 (t,  $J = 7.2$  Hz, 2H), 2.74 – 2.71 (m, 4H), 2.69 – 2.66 (m, 4H), 2.42 – 2.38 (m, 4H), 2.17 (s, 3H), 1.69 – 1.53 (m, 4H), 1.44 – 1.33 (m, 2H), 0.96 (t,  $J = 7.4$  Hz, 3H).  $^{13}C$  NMR (126 MHz, MeOD)  $\delta$  163.3, 161.6, 160.4, 106.5, 59.0, 56.2, 41.6, 32.9, 28.3, 26.0, 23.2, 21.3, 20.3, 14.3. MS (ESI-QTOF) for  $C_{16}H_{29}N_5S$   $[M + H]^+$  calculated 324.2216, found 324.2247.

***N*<sup>4</sup>-Butyl-6-methyl-5-(3-morpholinopropyl)pyrimidine-2,4-diamine (17u).**

Intermediate compound **16u**. 4-(Prop-2-yn-1-yl)morpholine was used as reagent. Yellow solid (50 mg, 82%).  $^1H$  NMR (500 MHz,  $CDCl_3$ )  $\delta$  5.33 (s, 1H), 4.85 (s, 2H), 3.76 (t,  $J = 4.6$  Hz, 4H),

3.59 (s, 2H), 3.45 – 3.36 (m, 2H), 2.62 (t,  $J = 4.6$  Hz, 4H), 2.33 (s, 3H), 1.61 – 1.51 (m, 2H), 1.45 – 1.33 (m, 2H), 0.95 (t,  $J = 7.4$  Hz, 3H).  $^{13}\text{C}$  NMR (126 MHz,  $\text{CDCl}_3$ )  $\delta$  167.5, 163.1, 160.8, 93.7, 91.1, 79.3, 67.0, 52.5, 48.6, 40.6, 31.9, 23.1, 20.2, 14.0. MS (ESI-QTOF) for  $\text{C}_{16}\text{H}_{25}\text{N}_5\text{O}$   $[\text{M} + \text{H}]^+$  calculated 304.2132, found 304.2147.

Compound **17u**. White solid (24 mg, 78%).  $^1\text{H}$  NMR (500 MHz,  $\text{CDCl}_3$ )  $\delta$  6.45 (s, 1H), 4.79 (s, 2H), 3.76 – 3.74 (m, 4H), 3.40 – 3.36 (m, 2H), 2.47 – 2.41 (m, 4H), 2.39 (t,  $J = 6.7$  Hz, 2H), 2.28 (t,  $J = 6.4$  Hz, 2H), 2.22 (s, 3H), 1.73 – 1.63 (m, 2H), 1.60 – 1.50 (m, 2H), 1.43 – 1.32 (m, 2H), 0.94 (t,  $J = 7.3$  Hz, 3H).  $^{13}\text{C}$  NMR (126 MHz,  $\text{CDCl}_3$ )  $\delta$  162.8, 160.1, 159.9, 105.4, 67.1, 56.2, 53.5, 40.9, 32.4, 25.0, 21.6, 20.6, 20.4, 14.1. MS (ESI-QTOF) for  $\text{C}_{16}\text{H}_{29}\text{N}_5\text{O}$   $[\text{M} + \text{H}]^+$  calculated 308.2445, found 308.2472.

***N*<sup>4</sup>-Butyl-5-(3-((2-methoxyethyl)(methyl)amino)propyl)-6-methylpyrimidine-2,4-diamine (17v).**

Intermediate compound **16v**. *N*-(2-Methoxyethyl)-*N*-methylprop-2-yn-1-amine was used as reagent. Brownish oil (50 mg, 82%). MS (ESI-QTOF) for  $\text{C}_{16}\text{H}_{27}\text{N}_5\text{O}$   $[\text{M} + \text{H}]^+$  calculated 306.2288, found 306.2275.

Compound **17v**. Pale oil (24 mg, 77%).  $^1\text{H}$  NMR (500 MHz, MeOD)  $\delta$  3.52 (t,  $J = 5.5$  Hz, 2H), 3.38 (t,  $J = 7.2$  Hz, 2H), 3.34 (s, 3H), 2.59 (t,  $J = 5.5$  Hz, 2H), 2.44 – 2.39 (m, 4H), 2.26 (s, 3H), 2.16 (s, 3H), 1.67 – 1.53 (m, 4H), 1.45 – 1.33 (m, 2H), 0.96 (t,  $J = 7.4$  Hz, 3H).  $^{13}\text{C}$  NMR (126 MHz, MeOD)  $\delta$  163.4, 162.0, 161.1, 106.5, 71.4, 59.0, 57.8, 57.1, 43.1, 41.7, 32.9, 26.8, 23.3, 21.3, 20.5, 14.3. MS (ESI-QTOF) for  $\text{C}_{16}\text{H}_{31}\text{N}_5\text{O}$   $[\text{M} + \text{H}]^+$  calculated 310.2601, found 310.2608.



***N*<sup>4</sup>-Butyl-6-methyl-5-(4-morpholinobutyl)pyrimidine-2,4-diamine (17w).**

Intermediate compound **16w**. 4-(But-3-yn-1-yl)morpholine was used as reagent. Yellow solid (48 mg, 76%). MS (ESI-QTOF) for C<sub>17</sub>H<sub>27</sub>N<sub>5</sub>O [M + H]<sup>+</sup> calculated 318.2288, found 318.2324.

Compound **17w**. White solid (25 mg, 78%). <sup>1</sup>H NMR (500 MHz, MeOD) δ 3.71 – 3.68 (m, 4H), 3.38 (t, *J* = 7.2 Hz, 2H), 2.47 – 2.45 (m, 4H), 2.43 – 2.36 (m, 4H), 2.16 (s, 3H), 1.64 – 1.52 (m, 4H), 1.49 – 1.32 (m, 4H), 0.95 (t, *J* = 7.4 Hz, 3H). <sup>13</sup>C NMR (126 MHz, MeOD) δ 163.0, 162.0, 161.0, 106.8, 67.6, 59.9, 54.8, 41.5, 32.9, 27.4, 26.9, 25.6, 21.3, 20.6, 14.3. MS (ESI-QTOF) for C<sub>17</sub>H<sub>31</sub>N<sub>5</sub>O [M + H]<sup>+</sup> calculated 322.2601, found 322.2601.

**Human TLR7/8-specific reporter gene assays (NF-κB induction), and TLR-2/-3/-4/-5/-9**

**counter-screens:** The induction of NF-κB was quantified using human TLR-2/-3/-4/-5/-7/-8/-9-specific, rapid-throughput, liquid handler-assisted reporter gene assays as previously described by us.<sup>31, 32, 47, 48</sup> HEK293 cells stably co-transfected with the appropriate hTLR and secreted alkaline phosphatase (sAP) were maintained in HEK-Blue™ Selection medium. Stable expression of secreted alkaline phosphatase (sAP) under control of NF-κB/AP-1 promoters is inducible by appropriate TLR agonists, and extracellular sAP in the supernatant is proportional to NF-κB induction. Reporter cells were incubated at a density of ~10<sup>5</sup> cells/ml in a volume of 80 μl/well, in 384-well, flat-bottomed, cell culture-treated microtiter plates in the presence of graded concentrations of stimuli. sAP was assayed spectrophotometrically using an alkaline phosphatase-specific chromogen (present in HEK-detection medium as supplied by InvivoGen) at 620 nm.

**Multiplexed immunoassays for cytokines.** Fresh human peripheral blood mononuclear cells

(hPBMC) were isolated from human blood obtained by venipuncture in Cell Preparation Tubes (CPT, Beckton-Dickinson) with informed consent and as per guidelines approved by the University of Minnesota Human Subjects Experimentation Committee. Aliquots of PBMCs ( $10^5$  cells in 100  $\mu$ L/well) were stimulated for 16 h with graded concentrations of test compounds. Supernatants were isolated by centrifugation, and were assayed in duplicates using analyte-specific multiplexed cytokine/chemokine bead array assays (HCYTMAP-60K-PX41 MILLIPLEX MAP Human Cytokine/Chemokine Magnetic Bead Panel, EMD Millipore, Billerica, MA) as reported by us previously.<sup>42</sup> The following analytes were quantified: sCD40L, VEGF, TNF- $\beta$ , TNF- $\alpha$ , TGF- $\alpha$ , RANTES, PDGF-AB/BB, PDGF-AA, MIP-1 $\beta$ , MIP-1 $\alpha$ , MDC (CCL22), MCP-3, MCP-1, IP-10, IL-17A, IL-15, IL-13, IL-12 (p70), IL-12 (p40), IL-10, IL-9, IL-8, IL-7, IL-6, IL-5, IL-4, IL-3, IL-2, IL-1ra, IL-1 $\beta$ , IL-1 $\alpha$ , IFN- $\gamma$ , IFN- $\alpha$ 2, GRO, GM-CSF, G-CSF, fractalkine, Flt-3 ligand, FGF-2, eotaxin, EGF.

**IFN- $\alpha$ / $\beta$ , IFN- $\gamma$ , and TNF- $\alpha$ /IL-1 $\beta$  Whole Blood Reporter Gene Assays.** Whole heparinized blood was collected from consenting individuals as approved by the University of Minnesota Institutional Review Board, and was diluted 1:2 in RPMI supplemented with 10% fetal bovine serum (FBS). Forty  $\mu$ L was added to 384-well, flat-bottomed, cell culture-treated microtiter plates containing serial dilutions of compounds. Following incubation at 37°C for 24 h, 40  $\mu$ L of supernatant was transferred to separate 384-well plates using liquid handler equipped with liquid level sensing in order to avoid disturbing the erythrocyte-rich pellet. Forty  $\mu$ L of HEK-IFN $\alpha$ / $\beta$ , HEK-IFN $\gamma$ , or HEK-TNF $\alpha$ /IL-1 $\beta$  cytokine reporter cells (InvivoGen, San Diego, CA) harvested at a density of  $1 \times 10^6$  cells/mL in DMEM with 10% FBS were added to the supernatant plates and incubated at 37°C for 24 hours. The plates were washed in sterile PBS using a plate washer

(BioTek, Winooski, VT), and 40  $\mu$ L of HEK Blue Detection Media (InvivoGen, San Diego, CA) was added and incubated for 16 hours at 37°C. sAP was assayed spectrophotometrically using an alkaline phosphatase-specific chromogen (present in HEK-detection medium as supplied by InvivoGen) at 620 nm.

In order to calibrate the assays, human serum (or plasma) was ‘spiked’ with graded concentrations of human IFN- $\alpha$ , IFN- $\gamma$ , or TNF- $\alpha$ , and cytokine reporter assays were performed as described above. Sigmoidal dose-response profiles for each cytokine were observed (Fig. 4 and Fig. S3), from which threshold cytokine concentrations corresponding to maximal responses for each cytokine reporter cell line were recorded. Compound concentrations eliciting maximal cytokine responses were defined as Effective Concentrations eliciting Maximal Responses (ECMR<sub>100</sub>).

**Flow-cytometric immunostimulation experiments:** Cell surface marker upregulation was determined by flow cytometry using protocols published by us previously<sup>64</sup> and modified for rapid throughput. Briefly, PBMC samples were obtained by venipuncture in CPT Vacutainer tubes (Becton-Dickinson Biosciences, San Jose, CA) from healthy human volunteers with informed consent and as per guidelines approved by the University of Minnesota Institutional Review Board. Serial dilutions of selected compounds were performed using a Bio-Tek Precision 2000 XS liquid handler in sterile 96-well polypropylene plates, to which 100  $\mu$ L aliquots of PBMCs were added. The plates were incubated at 37 °C for 16 h. Negative (DMSO) controls were included in each experiment. The following fluorochrome-conjugated antibodies were used for pDCs: CD11c PerCP-Cy5.5 (BioLegend, San Diego, CA), CD304 BV421, CD123 BV510, Lin Cocktail FITC, CD80 PE, HLA-DR APC (Becton-Dickinson Biosciences, San Jose,

CA) and Fixable Viability Dye eFluor 780 (eBioscience, San Diego, CA), and for cDCs: CD1c BV421, CD141 BV510, Lin Cocktail FITC, CD80 PE, CD11c PerCP-Cy5.5, HLA-DR APC (Becton-Dickinson Biosciences, San Jose, CA) and Fixable Viability Dye eFluor 780 (eBioscience, San Diego, CA). Following incubation, PBMCs were washed with sterile PBS and stained with 1:1000 eFluor780 in PBS for 20 min at 4 °C. Viability staining was followed by washing with RPMI containing 10% FBS and 2.5 µg of each antibody was added to wells with a liquid handler and incubated at 4 °C in the dark for 30 min. Following staining PBMCs were fixed by mixing 200 µL of the samples in 800 µL prewarmed cytofix buffer (Becton-Dickinson Biosciences, San Jose, CA) in 96 deep-well plates. After washing the cells twice at 300 g for 10 min in RPMI, the cells were transferred to a 96-well plate. Flow cytometry was performed using a BD FACSVerse instrument for acquisition on 250,000 gated events. Compensation for spillover was computed for each experiment on singly stained UltraComp Beads (eBioscience, San Diego, CA). Fluorescence minus one (FMO) and isotype controls were used to identify DC populations.<sup>69-71</sup> pDCs were defined as Live, Lin<sup>-</sup>, CD123<sup>+</sup>, CD303<sup>+</sup>, CD304<sup>+</sup>, HLA-DR<sup>+</sup>. CD141<sup>+</sup> cDCs were defined as Live, Lin<sup>-</sup>, CD1c<sup>-</sup>, CD141<sup>+</sup>, HLA-DR<sup>+</sup>. CD1c<sup>+</sup> cDC were defined as Live, Lin<sup>-</sup>, CD141<sup>-</sup>, CD1c<sup>+</sup>, CD11c<sup>+</sup>, HLA-DR<sup>+</sup>. Median fluorescence intensities were quantified for each population using FlowJo, version 10.0, software (FlowJo, LLC, Ashland, OR).

**Statistical methods:** Data were analyzed and plotted using Origin Version 7 (OriginLab, Northampton, MA). P values for regression coefficients denote significance levels (two-tailed) for the t-test of the slope = 0.

**Supporting Information:** Characterization data ( $^1\text{H}$ ,  $^{13}\text{C}$ , mass spectra), LC-MS analyses of key precursors and final compounds. SMILE information and TLR7/8 agonistic activity for compounds **3**, **6a-b**, **10a**, **11a-d**, **12**, **13**, **14a-b**, **16a**, **16l**, **16u**, **17a-w** (CSV).

**Corresponding Author Address:**

Sunil A. David,

Department of Medicinal Chemistry,

2-132, Cancer & Cardiovascular Research Building, 2231 6th St. SE.,

University of Minnesota, Minneapolis, MN 55455.

Tel: 612-625-3317; Email: [sdavid@umn.edu](mailto:sdavid@umn.edu)

**Acknowledgments:** This work was supported by NIH/NIAID contract HHSN272201400056C.

**Abbreviations:** APCs, Antigen-presenting cells; CD, Cluster of differentiation; cDC, conventional dendritic cell; DIPEA, *N,N*-diisopropylethylamine; ECMR<sub>100</sub>; Effective Concentrations eliciting Maximal Responses; ESI-QTOF, Electrospray ionization-quadrupole time of flight; EC<sub>50</sub>, Half-maximal effective concentration; HEK, Human embryonic kidney; HLA-DR, Human Leukocyte Antigen-antigen D Related; IFN, Interferon; IL, Interleukin; MPLA, monophosphoryl lipid A; NIS, *N*-iodosuccinimide; mDC, myeloid dendritic cell; PAMPs, pathogen-associated molecular patterns; PBMCs, Peripheral blood mononuclear cells; pDC, plasmacytoid dendritic cell; NF- $\kappa$ B, Nuclear factor- $\kappa$ B; PRRs, pattern-recognition receptors; sAP, Secreted alkaline phosphatase; Th1, Helper T lymphocyte-type 1; Th2, Helper T lymphocyte-type 2; Th9, Helper T lymphocyte-type 9; Th17, Helper T lymphocyte-type 17; TLR, Toll-like receptor; TNF- $\alpha$ , Tumor necrosis factor- $\alpha$ .

## References

1. Andre, F. E.; Booy, R.; Bock, H. L.; Clemens, J.; Datta, S. K.; John, T. J.; Lee, B. W.; Lolekha, S.; Peltola, H.; Ruff, T. A.; Santosham, M.; Schmitt, H. J. Vaccination greatly reduces disease, disability, death and inequity worldwide. *Bull. W. H. O.* **2008**, *86*, 140-146.
2. Levine, M. M.; Robins-Browne, R. Vaccines, global health and social equity. *Immunol. Cell Biol.* **2009**, *87*, 274-278.
3. Tambo, E.; Chuisseu, P. D.; Ngogang, J. Y.; Khater, E. I. Deciphering emerging zika and dengue viral epidemics: Implications for global maternal-child health burden. *J. Infect. Public Health* **2016**, *9*, 240-250.
4. Pierson, T. C.; Graham, B. S. Zika Virus: Immunity and vaccine development. *Cell* **2016**, *167*, 625-631.
5. Mayer, S. V.; Tesh, R. B.; Vasilakis, N. The emergence of arthropod-borne viral diseases: A global prospective on dengue, chikungunya and zika fevers. *Acta Trop.* **2016**, *166*, 155-163.
6. Lo Presti, A.; Cella, E.; Angeletti, S.; Ciccozzi, M. Molecular epidemiology, evolution and phylogeny of chikungunya virus: An updating review. *Infect. Genet. Evol.* **2016**, *41*, 270-278.
7. Aziz, H.; Zia, A.; Anwer, A.; Aziz, M.; Fatima, S.; Faheem, M. Zika virus: Global health challenge, threat and current situation. *J. Med. Virol.* **2016**. 10.1002/jmv.24731.
8. Medzhitov, R.; Janeway, C. A., Jr. Innate immune recognition and control of adaptive immune responses. *Semin. Immunol.* **1998**, *10*, 351-353.

9. Janeway, C. A. J. Presidential address to the american association of immunologists. The road less traveled by: the role of innate immunity in the adaptive immune response. *J. Immunol.* **1998**, *161*, 539-544.
10. Janeway, C. A., Jr.; Medzhitov, R. Innate immune recognition. *Annu. Rev. Immunol.* **2002**, *20*, 197-216.
11. Medzhitov, R.; Janeway, C. A. J. Innate immunity. *New Engl. J. Med.* **2000**, *343*, 338-344.
12. O'Hagan, D. T.; Fox, C. B. New generation adjuvants--from empiricism to rational design. *Vaccine* **2015**, *33 Suppl 2*, B14-20.
13. Gellin, B. G.; Salisbury, D. M. Communicating the role and value of vaccine adjuvants. *Vaccine* **2015**, *33 Suppl 2*, B44-46.
14. Di Pasquale, A.; Preiss, S.; Tavares Da Silva, F.; Garcon, N. Vaccine adjuvants: from 1920 to 2015 and beyond. *Vaccines* **2015**, *3*, 320-343.
15. Apostolico Jde, S.; Lunardelli, V. A.; Coirada, F. C.; Boscardin, S. B.; Rosa, D. S. Adjuvants: Classification, modus operandi, and licensing. *J. Immunol. Res.* **2016**, *2016*, 1459394.
16. Beutler, B.; Hoebe, K.; Du, X.; Ulevitch, R. J. How we detect microbes and respond to them: the Toll-like receptors and their transducers. *J. Leukoc. Biol.* **2003**, *74*, 479-485.
17. Kumagai, Y.; Akira, S. Identification and functions of pattern-recognition receptors. *J. Allergy Clin. Immunol.* **2010**, *125*, 985-992.
18. Kawai, T.; Akira, S. The role of pattern-recognition receptors in innate immunity: update on Toll-like receptors. *Nat. Immunol.* **2010**, *11*, 373-384.

19. Gay, N. J.; Gangloff, M.; Weber, A. N. Toll-like receptors as molecular switches. *Nat. Rev. Immunol.* **2006**, *6*, 693-698.
20. Takeda, K.; Akira, S. Toll-like receptors. *Curr. Protoc. Immunol.* **2015**, *109*, 14.12.1-14.12.10.
21. Pandey, S.; Kawai, T.; Akira, S. Microbial sensing by Toll-like receptors and intracellular nucleic acid sensors. *Cold Spring Harb. Perspect. Biol.* **2014**, *7*, a016246.
22. Song, D. H.; Lee, J. O. Sensing of microbial molecular patterns by Toll-like receptors. *Immunol. Rev.* **2012**, *250*, 216-229.
23. Gao, D.; Li, W. Structures and recognition modes of toll-like receptors. *Proteins* **2016**. doi: 10.1002/prot.25179.
24. Agnihotri, G.; Crall, B. M.; Lewis, T. C.; Day, T. P.; Balakrishna, R.; Warshakoon, H. J.; Malladi, S. S.; David, S. A. Structure-activity relationships in Toll-like receptor 2-agonists leading to simplified monoacyl lipopeptides. *J. Med. Chem.* **2011**, *54*, 8148-8160.
25. Salunke, D. B.; Connelly, S. W.; Shukla, N. M.; Hermanson, A. R.; Fox, L. M.; David, S. A. Design and development of stable, water-soluble, human Toll-like receptor 2 specific monoacyl lipopeptides as candidate vaccine adjuvants. *J. Med. Chem.* **2013**, *56*, 5885-5900.
26. Salunke, D. B.; Shukla, N. M.; Yoo, E.; Crall, B. M.; Balakrishna, R.; Malladi, S. S.; David, S. A. Structure-activity relationships in human Toll-like receptor 2-specific monoacyl lipopeptides. *J. Med. Chem.* **2012**, *55*, 3353-3363.
27. Salyer, A. C.; Caruso, G.; Khetani, K. K.; Fox, L. M.; Malladi, S. S.; David, S. A. Identification of adjuvant activity of amphotericin B in a novel, multiplexed, poly-TLR/NLR high-throughput screen. *PloS One* **2016**, *11*, e0149848.



28. Adediran, S. A.; Day, T. P.; Sil, D.; Kimbrell, M. R.; Warshakoon, H. J.; Malladi, S. S.; David, S. A. Synthesis of a highly water-soluble derivative of amphotericin B with attenuated proinflammatory activity. *Mol.Pharm.* **2009**, *6*, 1582-1590.
29. Shukla, N. M.; Kimbrell, M. R.; Malladi, S. S.; David, S. A. Regioisomerism-dependent TLR7 agonism and antagonism in an imidazoquinoline. *Bioorg. Med. Chem. Lett.* **2009**, *19*, 2211-2214.
30. Shukla, N. M.; Lewis, T. C.; Day, T. P.; Mutz, C. A.; Ukani, R.; Hamilton, C. D.; Balakrishna, R.; David, S. A. Toward self-adjuvanting subunit vaccines: model peptide and protein antigens incorporating covalently bound toll-like receptor-7 agonistic imidazoquinolines. *Bioorg. Med. Chem. Lett.* **2011**, *21*, 3232-3236.
31. Shukla, N. M.; Malladi, S. S.; Day, V.; David, S. A. Preliminary evaluation of a 3H imidazoquinoline library as dual TLR7/TLR8 antagonists. *Bioorg. Med. Chem.* **2011**, *19*, 3801-3811.
32. Shukla, N. M.; Malladi, S. S.; Mutz, C. A.; Balakrishna, R.; David, S. A. Structure-activity relationships in human toll-like receptor 7-active imidazoquinoline analogues. *J. Med. Chem.* **2010**, *53*, 4450-4465.
33. Shukla, N. M.; Mutz, C. A.; Malladi, S. S.; Warshakoon, H. J.; Balakrishna, R.; David, S. A. Toll-like receptor (TLR)-7 and -8 modulatory activities of dimeric imidazoquinolines. *J. Med. Chem.* **2012**, *55*, 1106-1116.
34. Shukla, N. M.; Mutz, C. A.; Ukani, R.; Warshakoon, H. J.; Moore, D. S.; David, S. A. Syntheses of fluorescent imidazoquinoline conjugates as probes of Toll-like receptor 7. *Bioorg. Med. Chem. Lett.* **2010**, *20*, 6384-6386.

35. Shukla, N. M.; Salunke, D. B.; Balakrishna, R.; Mutz, C. A.; Malladi, S. S.; David, S. A. Potent adjuvanticity of a pure TLR7-agonistic imidazoquinoline dendrimer. *PloS One* **2012**, *7*, e43612.
36. Yoo, E.; Salunke, D. B.; Sil, D.; Guo, X.; Salyer, A. C.; Hermanson, A. R.; Kumar, M.; Malladi, S. S.; Balakrishna, R.; Thompson, W. H.; Tanji, H.; Ohto, U.; Shimizu, T.; David, S. A. Determinants of activity at human Toll-like receptors 7 and 8: quantitative structure-activity relationship (QSAR) of diverse heterocyclic scaffolds. *J. Med. Chem.* **2014**, *57*, 7955-7970.
37. Yoo, E.; Crall, B. M.; Balakrishna, R.; Malladi, S. S.; Fox, L. M.; Hermanson, A. R.; David, S. A. Structure-activity relationships in Toll-like receptor 7 agonistic 1H-imidazo[4,5-*c*]pyridines. *Org. Biomol. Chem.* **2013**, *11*, 6526-6545.
38. Beesu, M.; Kokatla, H. P.; David, S. A. Syntheses of human TLR8-specific small-molecule agonists. *Methods Mol. Biol.* **2017**, *1494*, 29-44.
39. Beesu, M.; Salyer, A. C.; Trautman, K. L.; Hill, J. K.; David, S. A. Human Toll-like Receptor (TLR) 8-specific agonistic activity in substituted pyrimidine-2,4-diamines. *J. Med. Chem.* **2016**, *59*, 8082-8093.
40. Beesu, M.; Malladi, S. S.; Fox, L. M.; Jones, C. D.; Dixit, A.; David, S. A. Human Toll-like receptor 8-selective agonistic activities in 1-alkyl-1H-benzimidazol-2-amines. *J. Med. Chem.* **2014**, *57*, 7325-7341.
41. Beesu, M.; Caruso, G.; Salyer, A. C.; Khetani, K. K.; Sil, D.; Weerasinghe, M.; Tanji, H.; Ohto, U.; Shimizu, T.; David, S. A. Structure-based design of human TLR8-specific agonists with augmented potency and adjuvanticity. *J. Med. Chem.* **2015**, *58*, 7833-7849.
42. Beesu, M.; Caruso, G.; Salyer, A. C.; Shukla, N. M.; Khetani, K. K.; Smith, L. J.; Fox, L. M.; Tanji, H.; Ohto, U.; Shimizu, T.; David, S. A. Identification of a human Toll-like receptor

(TLR) 8-specific agonist and a functional pan-TLR inhibitor in 2-aminoimidazoles. *J. Med.*

*Chem.* **2016**, *59*, 3311-3330.

43. Kokatla, H. P.; Sil, D.; Malladi, S. S.; Balakrishna, R.; Hermanson, A. R.; Fox, L. M.;

Wang, X.; Dixit, A.; David, S. A. Exquisite selectivity for human Toll-like receptor 8 in substituted furo[2,3-*c*]quinolines. *J. Med. Chem.* **2013**, *56*, 6871-6885.

44. Kokatla, H. P.; Yoo, E.; Salunke, D. B.; Sil, D.; Ng, C. F.; Balakrishna, R.; Malladi, S.

S.; Fox, L. M.; David, S. A. Toll-like receptor-8 agonistic activities in C2, C4, and C8 modified thiazolo[4,5-*c*]quinolines. *Org. Biomol. Chem.* **2013**, *11*, 1179-1198.

45. Kokatla, H. P.; Sil, D.; Tanji, H.; Ohto, U.; Malladi, S. S.; Fox, L. M.; Shimizu, T.;

David, S. A. Structure-based design of novel human Toll-like receptor 8 agonists.

*ChemMedChem* **2014**, *9*, 719-723.

46. Salunke, D. B.; Yoo, E.; Shukla, N. M.; Balakrishna, R.; Malladi, S. S.; Serafin, K. J.;

Day, V. W.; Wang, X.; David, S. A. Structure-activity relationships in human Toll-like receptor 8-active 2,3-diamino-furo[2,3-*c*]pyridines. *J. Med. Chem.* **2012**, *55*, 8137-8151.

47. Agnihotri, G.; Ukani, R.; Malladi, S. S.; Warshakoon, H. J.; Balakrishna, R.; Wang, X.;

David, S. A. Structure-activity relationships in nucleotide oligomerization domain 1 (Nod1) agonistic gamma-glutamyl-diaminopimelic acid derivatives. *J. Med. Chem.* **2011**, *54*, 1490-1510.

48. Ukani, R.; Lewis, T. C.; Day, T. P.; Wu, W.; Malladi, S. S.; Warshakoon, H. J.; David, S.

A. Potent adjuvant activity of a CCR1-agonistic bis-quinoline. *Bioorg. Med. Chem. Lett.* **2012**, *22*, 293-295.

49. Stevens, T. L.; Bossie, A.; Sanders, V. M.; Fernandez-Botran, R.; Coffman, R. L.;

Mosmann, T. R.; Vitetta, E. S. Regulation of antibody isotype secretion by subsets of antigen-specific helper T cells. *Nature.* **1988**, *334*, 255-258.

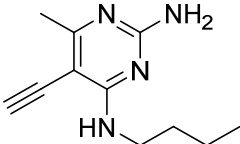
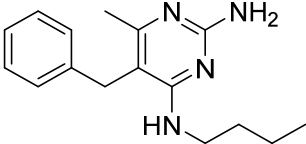
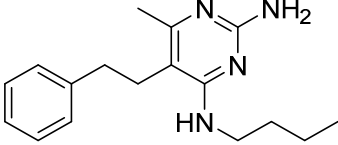
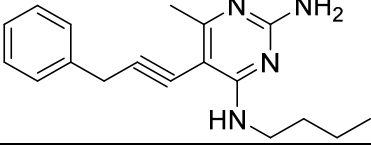
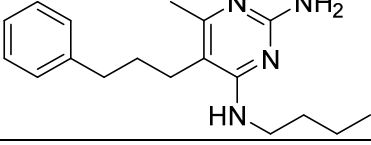
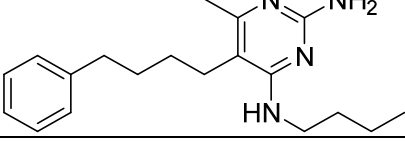
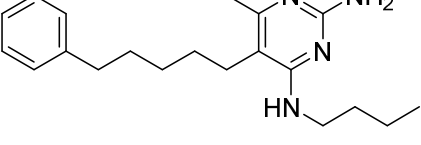
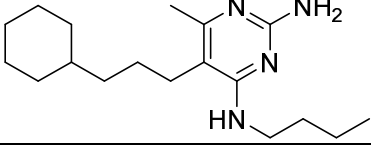
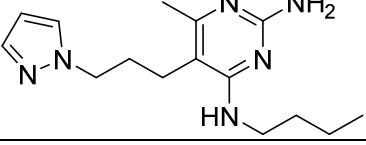
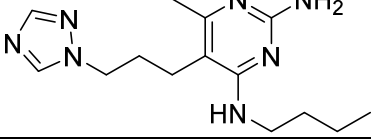
- 1  
2  
3 50. Mosmann, T. R.; Coffman, R. L. TH1 and TH2 cells: different patterns of lymphokine  
4 secretion lead to different functional properties. *Annu. Rev. Immunol.* **1989**, *7*, 145-173.  
5  
6  
7  
8 51. Coffman, R. L.; Mosmann, T. R. Isotype regulation by helper T cells and lymphokines.  
9  
10 *Monogr. Allergy.* **1988**, *24*, 96-103.  
11  
12 52. Hirahara, K.; Nakayama, T. CD4+ T-cell subsets in inflammatory diseases: beyond the  
13 Th1/Th2 paradigm. *Int. Immunol.* **2016**, *28*, 163-171.  
14  
15 53. Liu, Y. J. IPC: professional type 1 interferon-producing cells and plasmacytoid dendritic  
16 cell precursors. *Annu. Rev. Immunol.* **2005**, *23*, 275-306.  
17  
18 54. Kaisho, T. Pathogen sensors and chemokine receptors in dendritic cell subsets. *Vaccine*  
19  
20 **2012**, *30*, 7652-7657.  
21  
22 55. Gilliet, M.; Cao, W.; Liu, Y. J. Plasmacytoid dendritic cells: sensing nucleic acids in viral  
23 infection and autoimmune diseases. *Nat. Rev. Immunol.* **2008**, *8*, 594-606.  
24  
25 56. Cella, M.; Facchetti, F.; Lanzavecchia, A.; Colonna, M. Plasmacytoid dendritic cells  
26 activated by influenza virus and CD40L drive a potent TH1 polarization. *Nat. Immunol.* **2000**, *1*,  
27 305-310.  
28  
29 57. Huber, J. P.; Farrar, J. D. Regulation of effector and memory T-cell functions by type I  
30 interferon. *Immunol.* **2011**, *132*, 466-474.  
31  
32 58. Bekeredjian-Ding, I.; Roth, S. I.; Gilles, S.; Giese, T.; Ablasser, A.; Hornung, V.; Endres,  
33 S.; Hartmann, G. T cell-independent, TLR-induced IL-12p70 production in primary human  
34 monocytes. *J. Immunol.* **2006**, *176*, 7438-7446.  
35  
36 59. Warshakoon, H. J.; Hood, J. D.; Kimbrell, M. R.; Malladi, S.; Wu, W. Y.; Shukla, N. M.;  
37 Agnihotri, G.; Sil, D.; David, S. A. Potential adjuvant properties of innate immune stimuli.  
38  
39 *Hum. Vaccines* **2009**, *5*, 381-394.  
40  
41  
42  
43  
44  
45  
46  
47  
48  
49  
50  
51  
52  
53  
54  
55  
56  
57  
58  
59  
60

60. Bohnenkamp, H. R.; Papazisis, K. T.; Burchell, J. M.; Taylor-Papadimitriou, J. Synergism of Toll-like receptor-induced interleukin-12p70 secretion by monocyte-derived dendritic cells is mediated through p38 MAPK and lowers the threshold of T-helper cell type 1 responses. *Cell. Immunol.* **2007**, *247*, 72-84.
61. Philbin, V. J.; Levy, O. Immunostimulatory activity of Toll-like receptor 8 agonists towards human leucocytes: basic mechanisms and translational opportunities. *Biochem. Soc. Trans.* **2007**, *35*, 1485-1491.
62. Saruta, M.; Michelsen, K. S.; Thomas, L. S.; Yu, Q. T.; Landers, C. J.; Targan, S. R. TLR8-mediated activation of human monocytes inhibits TL1A expression. *Eur. J. Immunol.* **2009**, *39*, 2195-2202.
63. Wu, W.; Li, R.; Malladi, S. S.; Warshakoon, H. J.; Kimbrell, M. R.; Amolins, M. W.; Ukani, R.; Datta, A.; David, S. A. Structure-activity relationships in toll-like receptor-2 agonistic diacylthioglycerol lipopeptides. *J. Med. Chem.* **2010**, *53*, 3198-3213.
64. Hood, J. D.; Warshakoon, H. J.; Kimbrell, M. R.; Shukla, N. M.; Malladi, S.; Wang, X.; David, S. A. Immunoprofiling Toll-like receptor ligands: Comparison of immunostimulatory and proinflammatory profiles in ex vivo human blood models. *Hum. Vaccines* **2010**, *6*, 1-14.
65. Ganapathi, L.; Van Haren, S.; Dowling, D. J.; Bergelson, I.; Shukla, N. M.; Malladi, S. S.; Balakrishna, R.; Tanji, H.; Ohto, U.; Shimizu, T.; David, S. A.; Levy, O. The Imidazoquinoline Toll-like receptor-7/8 agonist hybrid-2 potently induces cytokine production by human newborn and adult leukocytes. *PloS one* **2015**, *10*, e0134640.
66. McGowan, D.; Herschke, F.; Pauwels, F.; Stoops, B.; Last, S.; Pieters, S.; Scholliers, A.; Thone, T.; Van Schoubroeck, B.; De Pooter, D.; Mostmans, W.; Khamlichi, M. D.; Embrechts, W.; Dhuyvetter, D.; Smyej, I.; Arnoult, E.; Demin, S.; Borghys, H.; Fanning, G.; Vlach, J.;

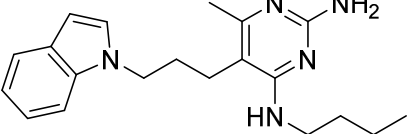
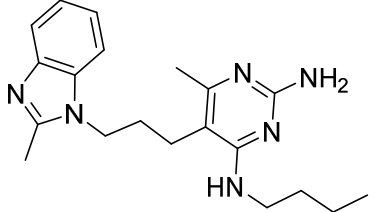
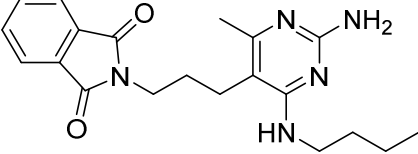
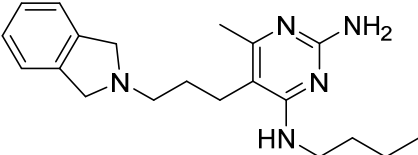
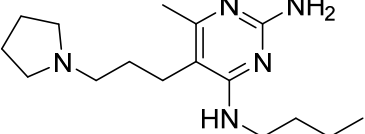
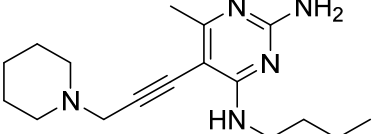
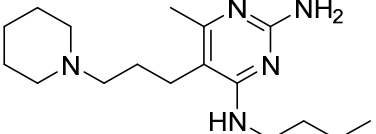
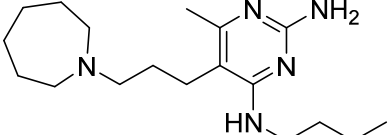
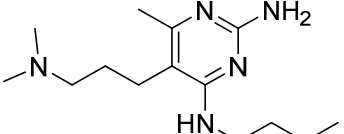
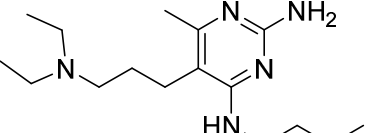
- Raboisson, P. Novel pyrimidine Toll-like receptor 7 and 8 dual agonists to treat hepatitis B virus. *J. Med. Chem.* **2016**, *59*, 7936-7949.
67. Selby, C. Interference in immunoassay. *Ann. Clin. Biochem.* **1999**, *36*, 704-721.
68. Jacobs, J. F.; van der Molen, R. G.; Bossuyt, X.; Damoiseaux, J. Antigen excess in modern immunoassays: to anticipate on the unexpected. *Autoimmun. Rev.* **2015**, *14*, 160-167.
69. MacDonald, K. P.; Munster, D. J.; Clark, G. J.; Dzionek, A.; Schmitz, J.; Hart, D. N. Characterization of human blood dendritic cell subsets. *Blood* **2002**, *100*, 4512-4520.
70. Dzionek, A.; Fuchs, A.; Schmidt, P.; Cremer, S.; Zysk, M.; Miltenyi, S.; Buck, D. W.; Schmitz, J. BDCA-2, BDCA-3, and BDCA-4: three markers for distinct subsets of dendritic cells in human peripheral blood. *J. Immunol.* **2000**, *165*, 6037-6046.
71. Dutertre, C. A.; Wang, L. F.; Ginhoux, F. Aligning bona fide dendritic cell populations across species. *Cell. Immunol.* **2014**, *291*, 3-10.

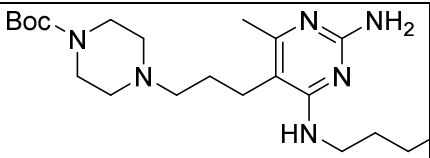
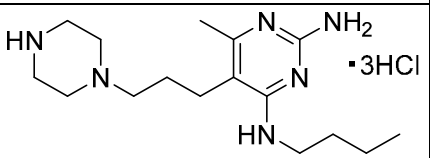
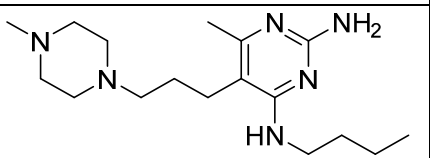
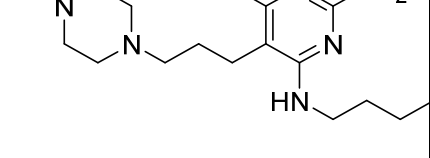
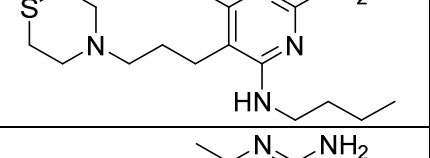
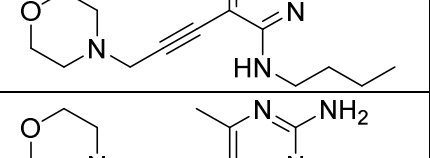
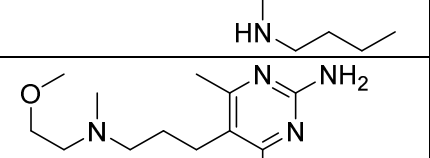
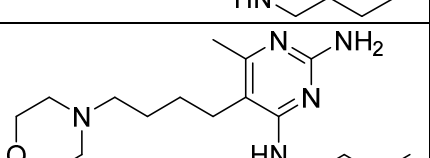
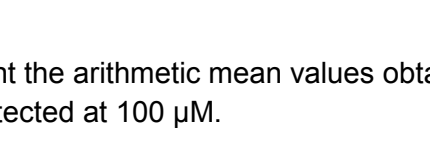
**Table 1. EC<sub>50</sub> values of compounds in human TLR7- and TLR8-specific reporter gene assays**

Compound Numbers	Structures	TLR7 Agonistic Activity (μM) <sup>a</sup>	TLR8 Agonistic Activity (μM) <sup>a</sup>
3		3.40	3.28
6a		1.27	1.66
6b		0.59	0.78
11a		0.51	1.22
11b		1.02	1.31
11c		3.26	3.14
11d		2.89	1.22
10a		Inactive	5.0
12		Inactive	9.24

13		Inactive	4.90
14a		Inactive	1.2
14b		2.82	1.19
16a		Inactive	Inactive
17a		0.194	0.749
17b		0.262	0.857
17c		0.265	0.830
17d		1.10	Inactive
17e		0.398	1.05
17f		1.16	1.05



17g		0.14	1.10
17h		0.379	0.366
17i		1.29	0.453
17j		0.375	0.029
17k		0.562	0.11
16l		Inactive	3.79
17l		0.71	0.133
17m		0.73	0.178
17n		0.958	0.126
17o		Inactive	0.254

17p		Inactive	0.30
17q		1.64	0.50
17r		0.251	0.179
17s		1.16	0.092
17t		0.714	0.167
16u		Inactive	16.2
17u		0.046	0.280
17v		1.24	0.203
17w		1.40	0.128

<sup>a</sup> EC<sub>50</sub> values represent the arithmetic mean values obtained on quadruplicate samples. Inactive denotes no activity detected at 100 μM.

## Legends to Figures

**Figure 1. Structures of key TLR7-, TLR8- and TLR7/TLR8-active compounds.**

**Figure 2. Agonistic activities of 2,4-diaminopyrimidine analogues in human TLR7 (A) and TLR8 (B) reporter gene assays.** Means  $\pm$  SD on quadruplicates are shown. Also included is **1c**, used as a reference TLR7/TLR8 dual active compound. The bimodal nature of agonistic responses resulting in apparent inhibition at high ligand concentrations was verified not to be due to cytotoxicity. None of these compounds were active in TLR-2/-3/-4/-5/-9 counter-screens (Figs. S1 and S2). C. Classification of analogues into inactive or weak active, dominant TLR8-active, and dual TLR7/TLR8-active based on arithmetic sum of responses at each concentration tested ( $\Sigma[R_{\text{conc.1}} + R_{\text{conc.2}} \dots + R_{\text{conc.n}}]$ ) at TLR7 and TLR8.

**Figure 3. Representative cytokine induction data in human PBMCs.** Means of duplicates are shown (excerpted from a 41 cytokine panel).

**Figure 4.** Induction of IFN- $\alpha/\beta$ , IFN- $\gamma$  and TNF- $\alpha$ /IL-1 $\beta$  in whole human blood by select compounds measured by cytokine reporter assays (complete datasets are shown in Fig. S3).

**Figure 5.** Correlation of TLR7 and TLR8 activity ( $\Sigma$ TLR response) in primary screens and EC<sub>50</sub> values of IFN- $\alpha/\beta$ , IFN- $\gamma$  and TNF- $\alpha$ /IL-1 $\beta$  induction in whole human blood, quantified using cytokine reporter assays.

**Figure 6. Gating strategy for the interrogation of DC populations by polychromatic flow**

cytometry. **A.** PBMCs were initially gated from FSC and SSC. **B.** Next, live/dead stain eFluor780 was used in combination with a lineage cocktail (CD3, CD14, CD16, CD19, CD20, CD56) to exclude non-dendritic cells and dead cells. **C.** CD303<sup>+</sup> CD304<sup>+</sup> cells (red) were selected using fluorescent minus one controls (FMO, green and blue). **D.** HLA-DR<sup>+</sup> CD123<sup>+</sup> pDC (red) were gated using FMO controls (blue and green). **E.** In separate experiments, CD1c<sup>+</sup> (BDCA1) and CD141<sup>+</sup> (BDCA3) cDC populations were identified from the Live Lin<sup>-</sup> population using FMO controls (blue and green). **F.** CD1c<sup>+</sup> cDCs were definitively identified as HLA-DR<sup>+</sup> CD11c<sup>+</sup>. FMO controls are shown in blue and green. **G.** CD141<sup>+</sup> cDCs were definitively identified as HLA-DR<sup>+</sup> using FMO controls shown in blue and green. All DC populations were examined for CD80 PE median fluorescence intensity.

**Figure 7.** Dose-response profiles of CD80 upregulation in human peripheral blood-derived dendritic cell subsets (pDCs, CD141<sup>+</sup> cDCs, CD1c<sup>+</sup> cDCs) by select pyrimidine diamines.

Figure 1

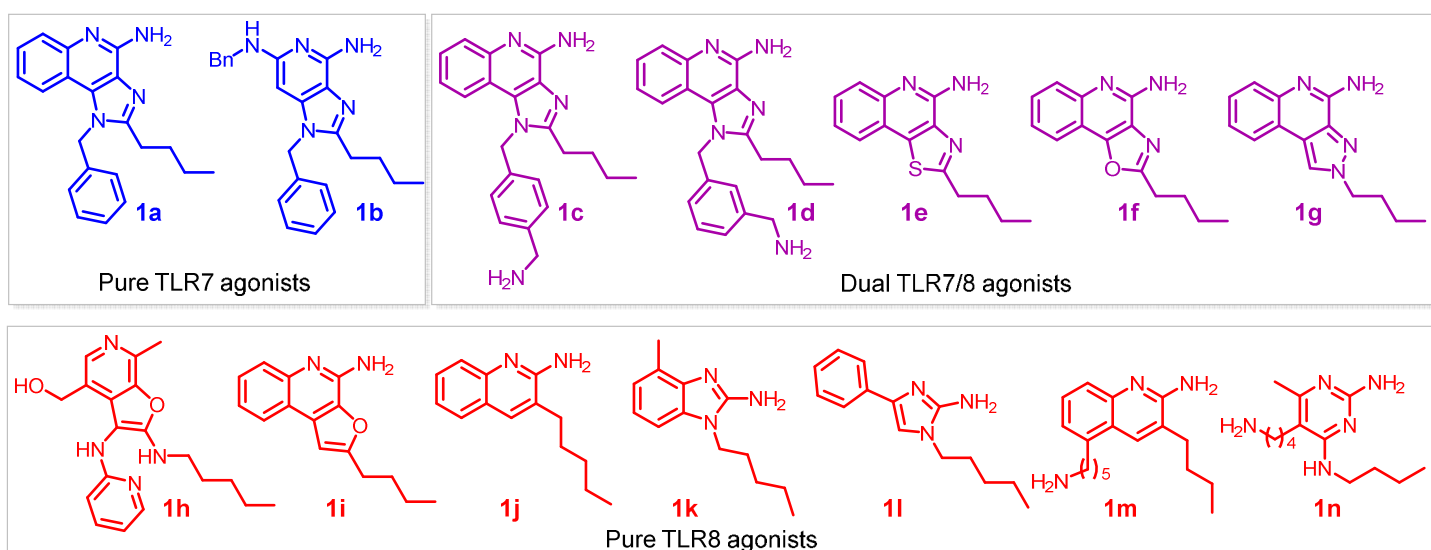


## Figure 2

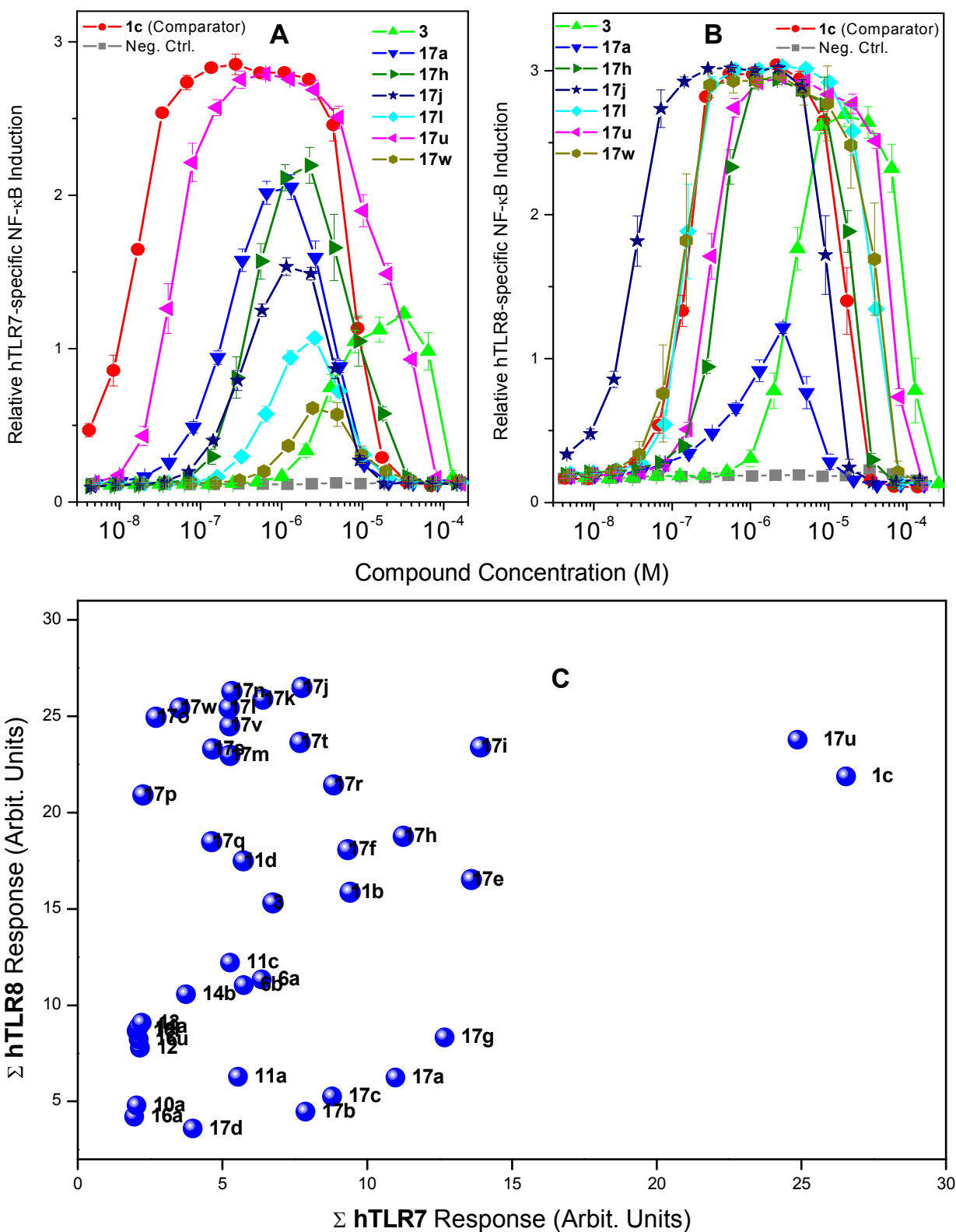


Figure 3

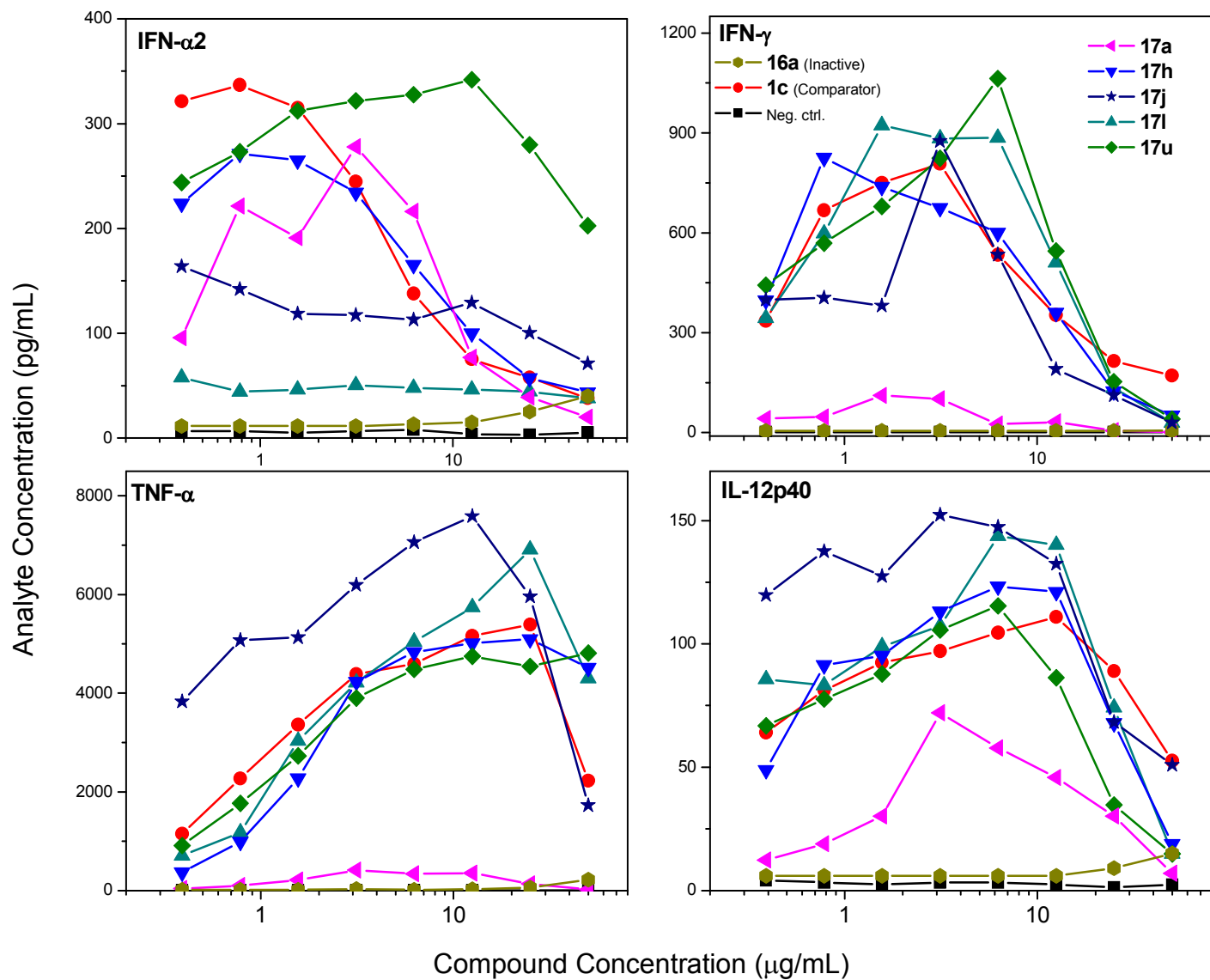
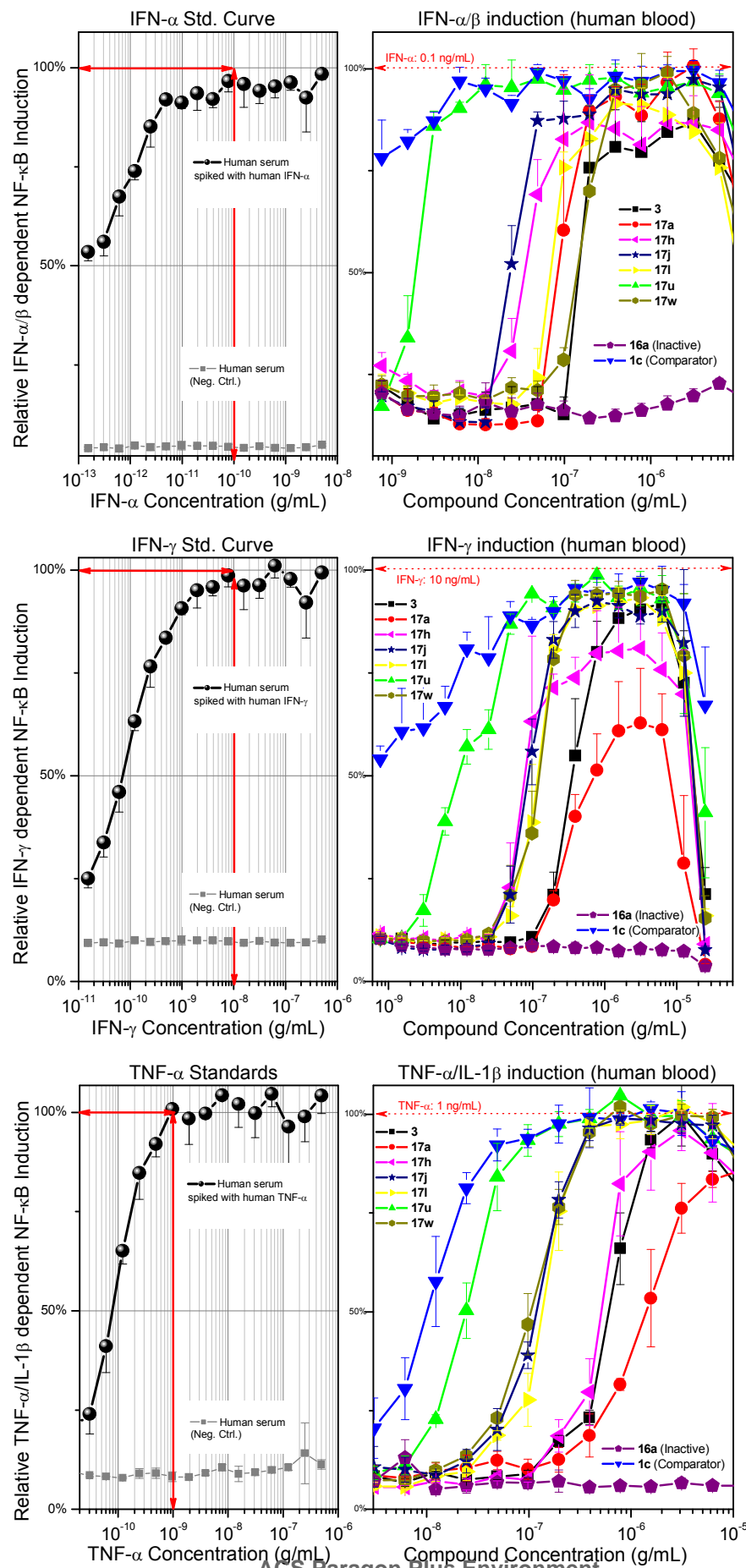


Figure 4





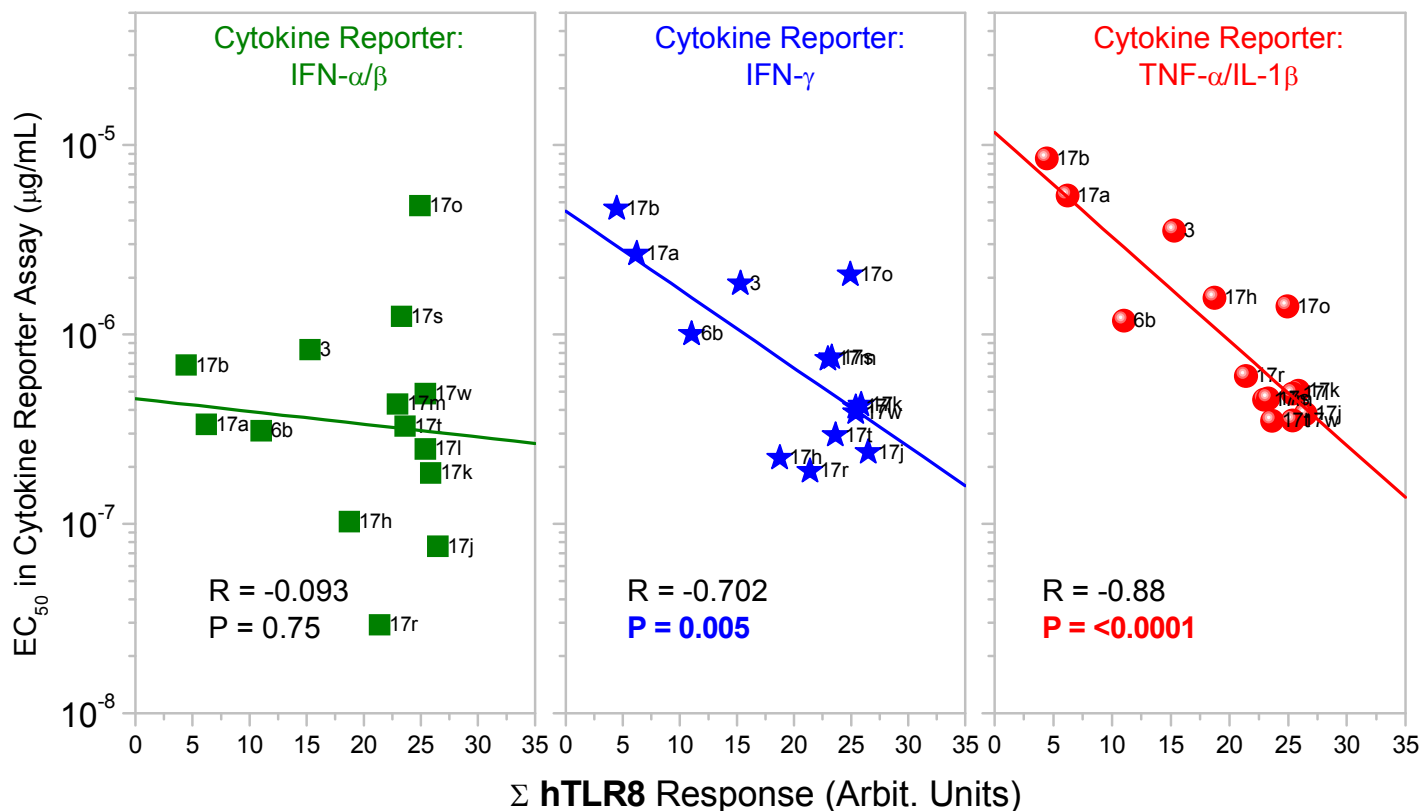
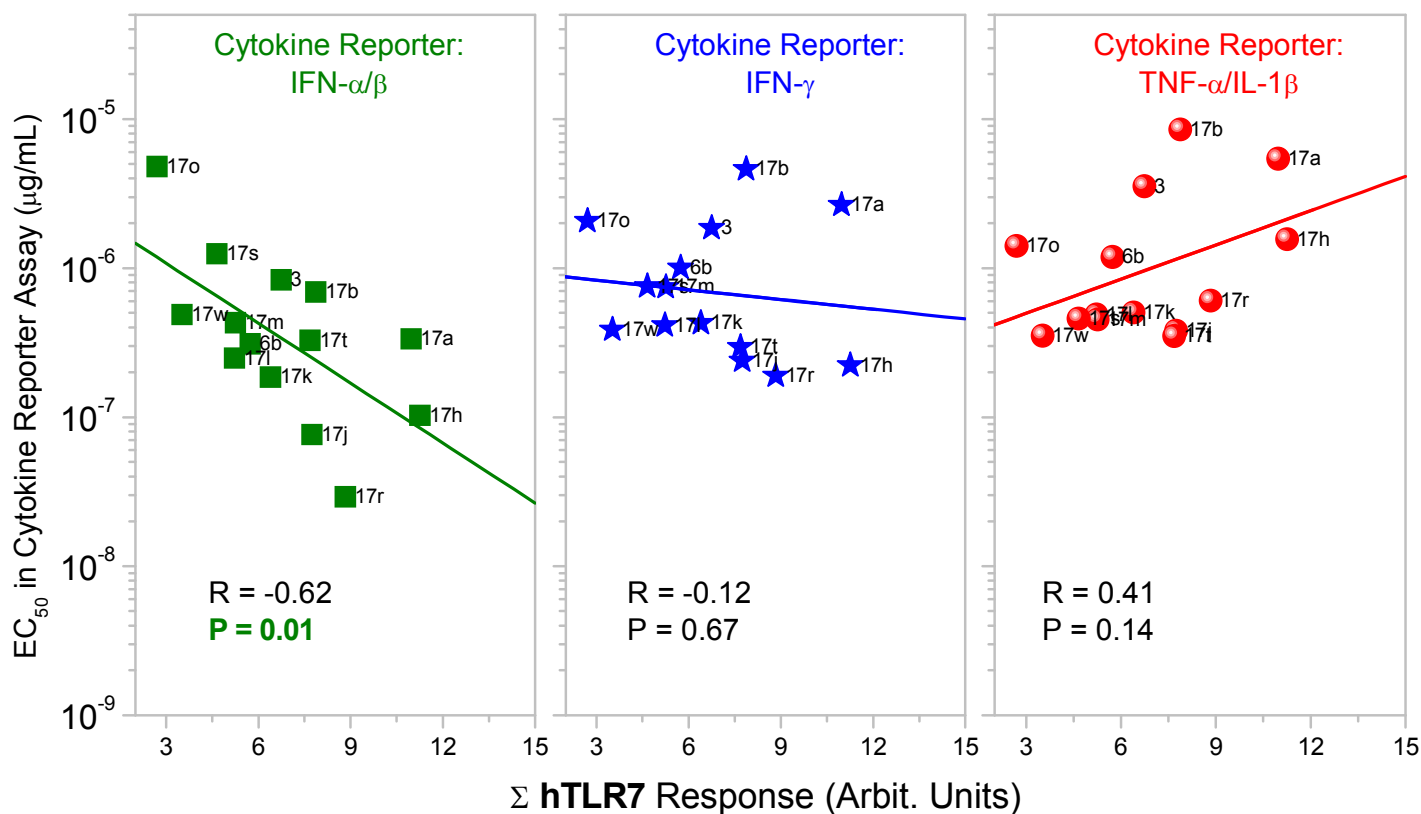


Figure 6

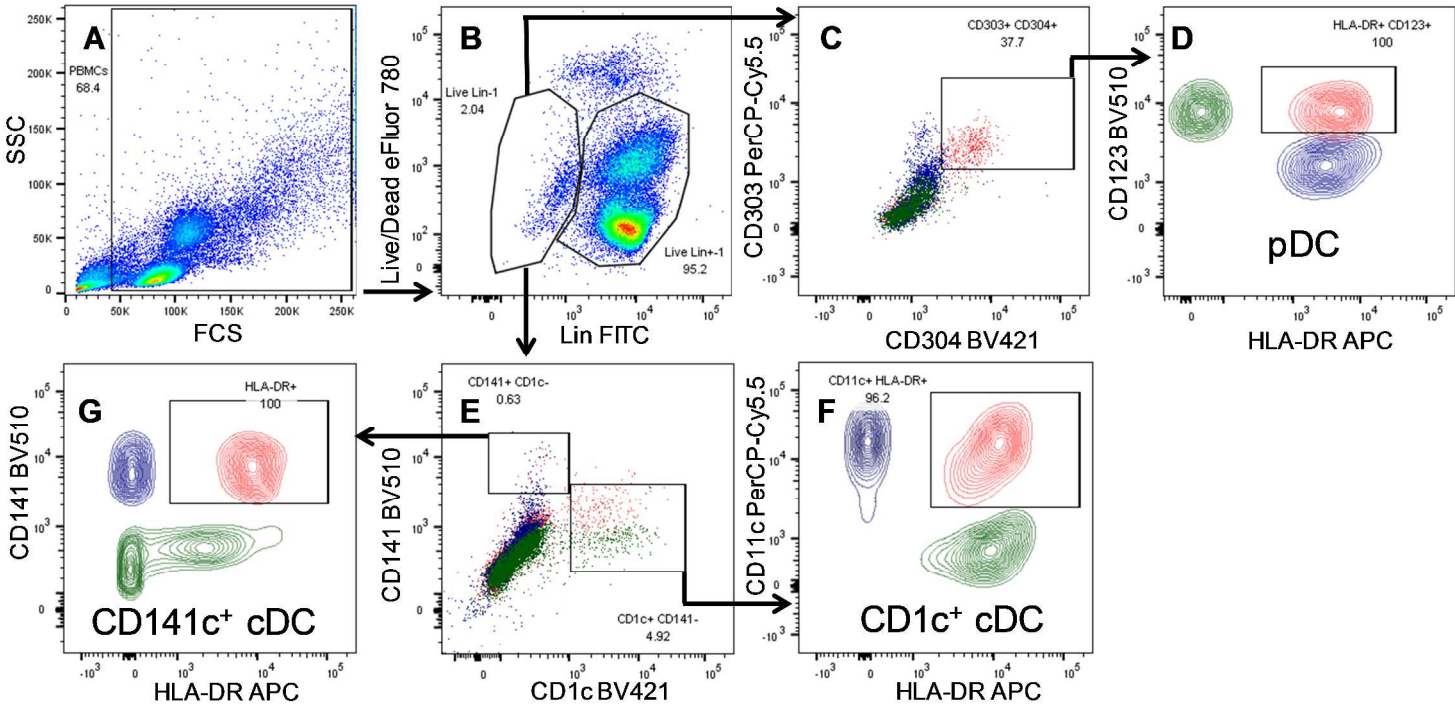
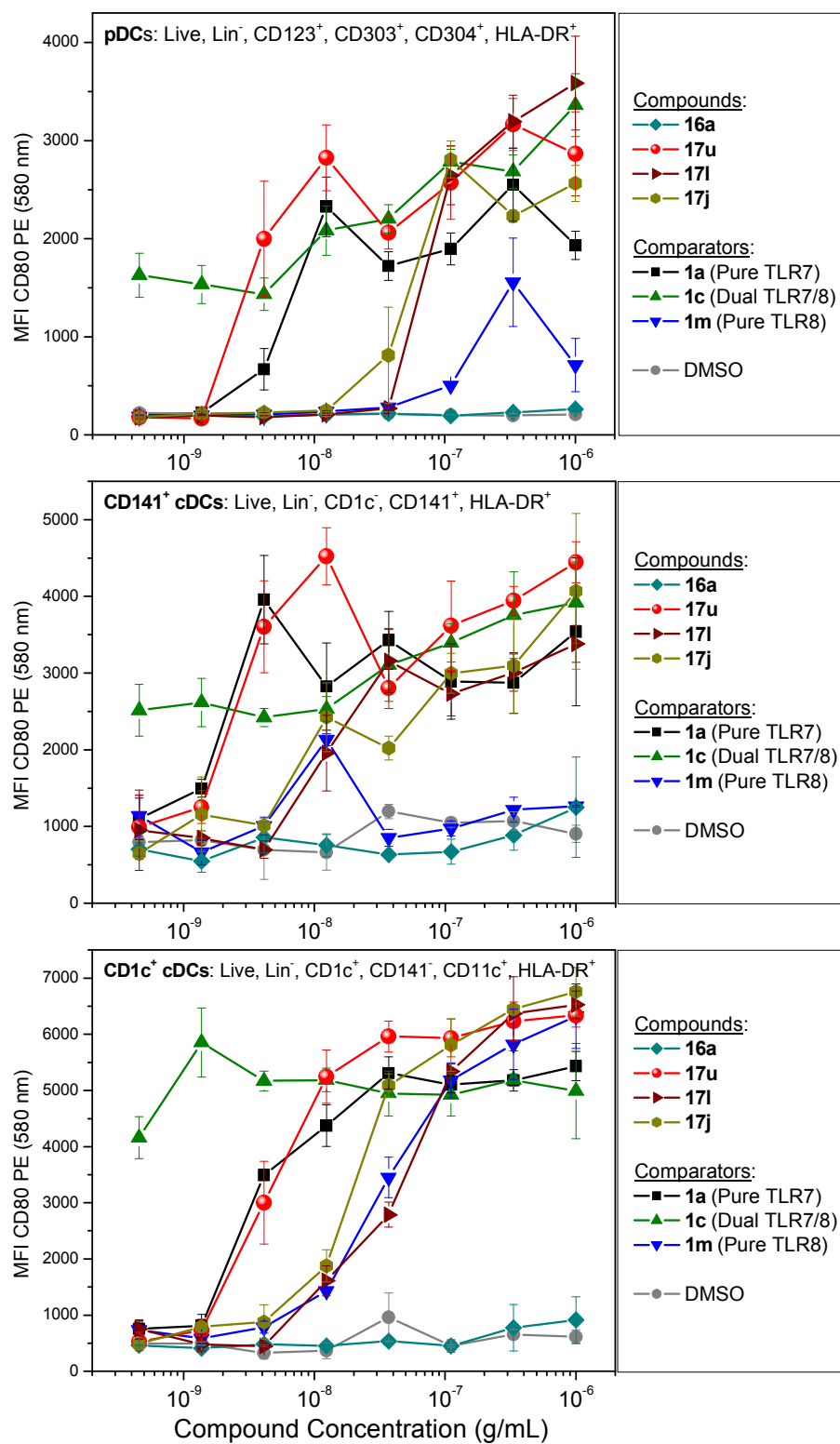
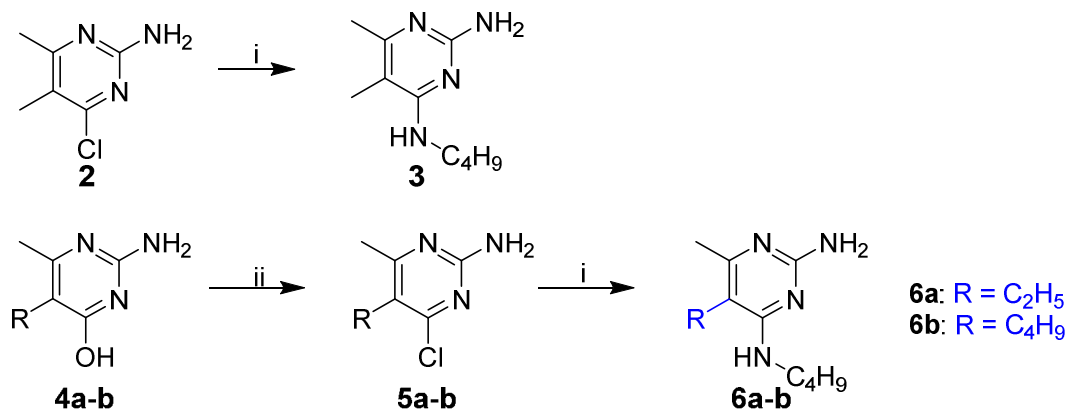


Figure 7

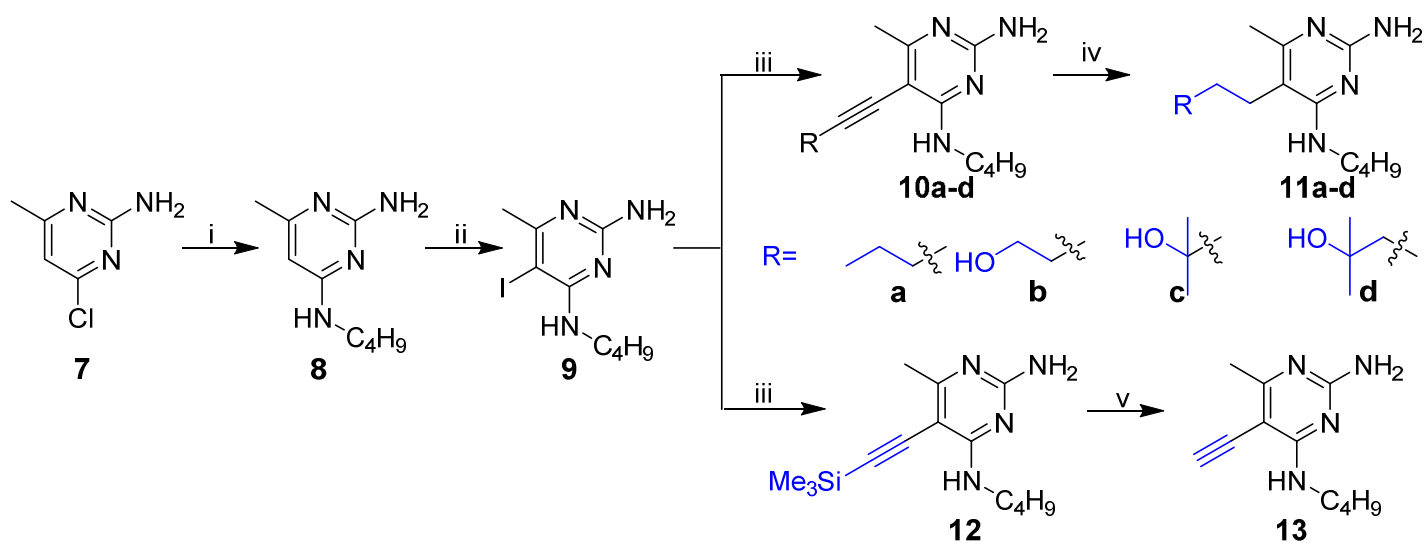


## Scheme 1



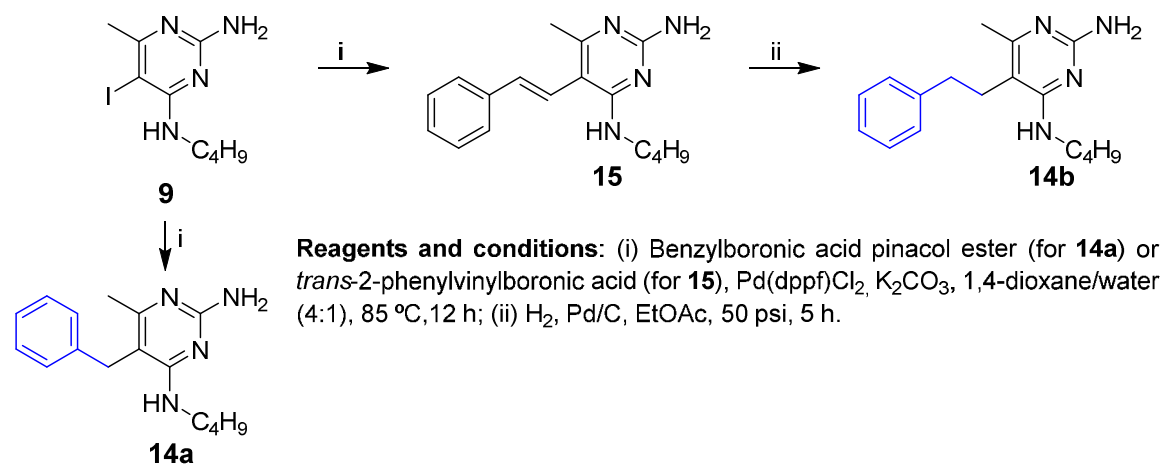
**Reagents and conditions:** (i) Butylamine, Et<sub>3</sub>N, MeOH, 70 °C, 12 h; (ii) POCl<sub>3</sub>, 85 °C, 3 h.

## Scheme 2

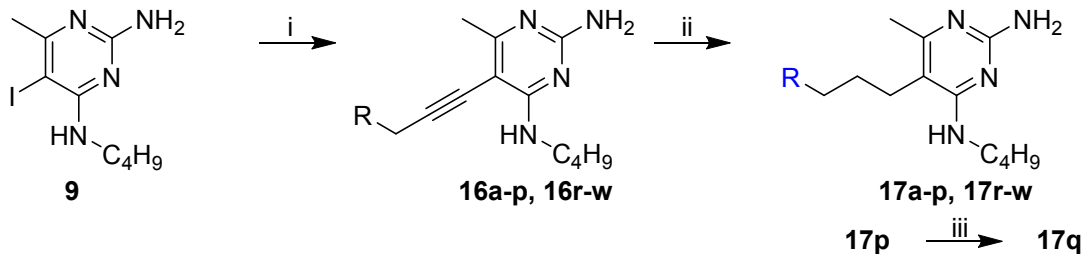


**Reagents and conditions:** (i) Butylamine, Et<sub>3</sub>N, MeOH, 70 °C, 12 h; (ii) NIS, DMF, 12 h; (iii) alkyne, Pd(PPh<sub>3</sub>)<sub>4</sub>, CuI, DIPEA/DMF (1:2), 12 h; (iv) H<sub>2</sub>, Pd/C, EtOAc, 50 psi, 5 h; (v) K<sub>2</sub>CO<sub>3</sub>, MeOH, 3 h.

## Scheme 3



Scheme 4



(i) Alkyne, Pd(PPh<sub>3</sub>)<sub>4</sub>, CuI, DIPEA/DMF (1:2), 12 h; (ii) H<sub>2</sub>, Pd/C, EtOAc, 50 psi, 5 h; (iii) HCl, 4 M, 3 h.

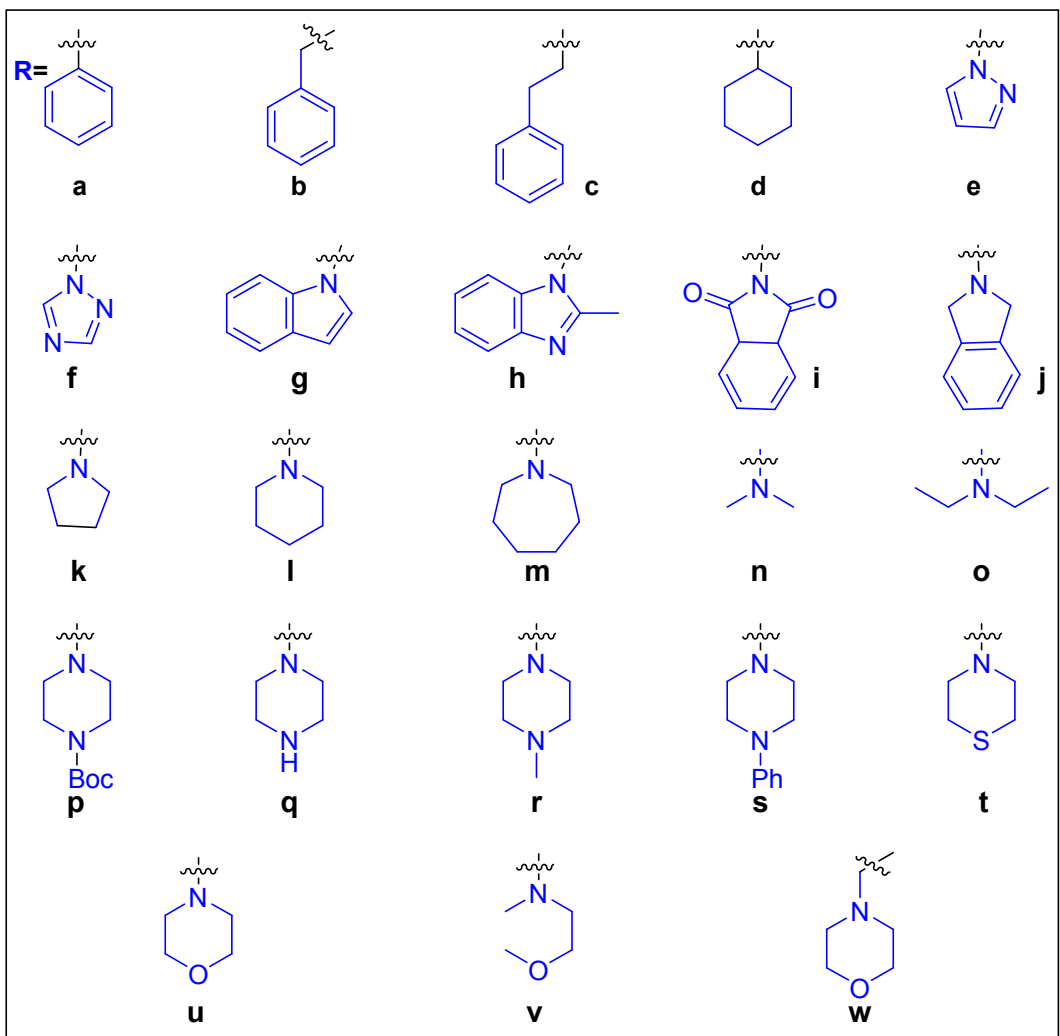


## Table of Contents Graphic

Height: 2.17" (5.5 cm)

Width: 2.88" (7.3 cm)

